



In Cooperation with the Southern Nevada Water Authority (SNWA)

Audiomagnetotelluric data from Spring, Cave, and Coyote Spring Valleys, Nevada

By Darcy K. McPhee, Bruce A. Chuchel, and Louise Pellerin

Open-File Report 2006–1164

U.S. Department of the Interior

U.S. Geological Survey

Contents

Abstract	1
Introduction	2
Audiomagnetotelluric Method	3
Audiomagnetotelluric Survey	5
Audiomagnetotelluric Data	6
Acknowledgments	8
References Cited	8

Figures

1. Topographic maps of study area showing locations of AMT profiles A, B, and E (A) and profile C (B).	10
--	----

Tables

1. Description of AMT profiles.	12
2. Sounding numbers, locations and elevations of stations along four AMT profiles	12

Appendix

A. Sounding curves	15
--------------------------	----

Audiomagnetotelluric data from Spring, Cave, and Coyote Spring Valleys, Nevada

By Darcy K. McPhee¹, Bruce A. Chuchel¹, and Louise Pellerin²

Abstract

Audiomagnetotelluric (AMT) data along four profiles in Spring, Cave, and Coyote Spring Valleys are presented here. The AMT method is used to estimate the electrical resistivity of the earth over depth ranges of a few meters to greater than one kilometer. This method is a valuable tool for revealing subsurface structure and stratigraphy within the Basin and Range of eastern Nevada, therefore helping to define the geohydrologic framework in this region. We collected AMT data using the Geometrics StrataGem EH4 system, a four-channel, natural and controlled-source tensor system recording in the range of 10 to 92,000 Hz. To augment the low signal in the natural field, an unpolarized transmitter comprised of two horizontal-magnetic dipoles was used from 1,000 to 70,000 Hz. Profiles were 1.4 – 12.6 km in length with station spacing of 100-400 m. Data were recorded with the electrical (E) field parallel to and perpendicular to the regional geologic strike direction. Station locations and sounding curves, showing apparent resistivity, phase data, and coherency data, are presented here.

¹ U.S. Geological Survey, 345 Middlefield Rd., MS 989, Menlo Park, CA 94025

² Green Engineering, Inc., 2215 Curtis St., Berkeley, CA 94702

Introduction

The Basin and Range province is an arid, mountainous, sparsely populated region of the western United States. Here, ground water is organized into extensive regional systems (Harrill and Prudic, 1998) where it can flow between adjacent topographic ranges and basins. Much of the structure that controls the hydrogeology of the valleys in eastern Nevada is obscured by sediments, hence geophysical investigations are underway to characterize the subsurface structures and stratigraphy influencing ground-water resources. The gravity method has been used to estimate the structure and depth of the basins in eastern Nevada (Mankinen et al., 2006; Scheirer, 2005), however densities of silicic ash-flow tuff units in the area may be comparable to the average density of basin sediment-fill causing difficulty in resolving the subsurface geometry between the basin-fill and volcanic rocks using the gravity method alone.

In this study, the audiomagnetotelluric (AMT) method was tested in Spring, Cave, and Coyote Spring valleys (Figure 1) to see if it is a feasible approach for mapping geologic/tectonic structures and thus could contribute significantly to the regional hydrological model in a typical Basin and Range setting. During the fall of 2004 and summer of 2005 AMT data were acquired along four profile lines (Figure 1). The AMT data obtained in this study were acquired to delineate range-front faults, structure, and stratigraphy within the basins as well as the geometry of the basins as a framework for hydrogeological modeling.

The purpose of this report is to release the AMT sounding data. No interpretation of the data is included.

Audiomagnetotelluric Method

The magnetotelluric (MT) method is a geophysical technique, which uses the earth's natural electromagnetic (EM) fields as a source to investigate the electrical resistivity structure of the subsurface (Vozoff, 1991). The resistivity of geologic units is largely dependent upon their fluid content, porosity, degree of fracturing, temperature, and conductive mineral content (Keller, 1989). Saline fluids within the pore spaces and fracture openings can reduce resistivities in a rock matrix. Resistivity can be lowered by the presence of conductive clay minerals, carbon, and metallic mineralization. Increased temperatures cause higher ionic mobility and mineral activation energy, reducing rock resistivities significantly. Unaltered, unfractured igneous rocks are normally very resistive, with values typically 1,000 ohm-m or greater. Fault zones can appear as low resistivity units of less than 100 ohm-m when they are comprised of rocks fractured enough to have hosted fluid transport and consequent mineralogical alteration (Eberhart-Phillips and others, 1995). Carbonate rocks are moderately to highly resistive, with values of hundreds to thousands of ohm-m depending upon their fluid content, porosity, fracturing, and impurities. Marine shale, mudstone, and clay-rich alluvium are normally very conductive – a few ohm-m to tens of ohm-m. Unaltered, metamorphic, non-graphitic rocks are moderately to highly resistive. Tables of electrical resistivity for a variety of rocks, minerals and geological environments may be found in Keller (1987) and Palacky (1987).

Using the same theory, the audiomagnetotelluric (AMT) method is used to estimate the electrical resistivity of the Earth over depth ranges of a few meters to greater than one kilometer (Zonge and Hughes, 1991). The Geometrics StrataGem EH-4 system, used in this study, utilizes both natural and man-made electromagnetic signals to obtain a continuous electrical sounding of the Earth beneath the measurement site (Geometrics, 2000). AMT systems are used to estimate the

electrical impedance at the Earth's surface from a series of simultaneous measurements of local electrical (E) and magnetic (H) field fluctuations made over a period of several minutes. The surface impedance is a complex function of frequency where higher-frequency data are influenced by shallow or nearby features, and lower-frequency data are influenced by structures at greater depth and distance. An AMT sounding provides an estimate of vertical resistivity beneath the receiver site and also indicates the geoelectric complexity at the sounding site. In areas where the resistivity distribution does not change rapidly from station to station, the resistivity sounding is a reasonable estimate of the geoelectric layering beneath the site.

The Stratagem system consists of two basic components; a receiver and a transmitter (Geometrics, 2000). The natural source is worldwide lightning, but in the frequency range above 1,000 Hz, natural signals are typically weak and a transmitter is used to augment the natural field and improve data quality. The unpolarized transmitter is comprised of two horizontal-magnetic dipoles and transmits signals from 1,000 to 70,000 Hz. The battery-powered system is compact and portable. Data are recorded in the range of 92,000 to 10 Hz. Surface impedance results are immediately displayed as a resistivity sounding. Data are subsequently modeled using two-dimensional inversion algorithms.

The natural electric and magnetic fields are measured in two orthogonal, horizontal directions. The tensor impedance, parameterized as apparent resistivity and phase, are obtained from the time-series signals. Signals are converted to complex cross-spectra using a Fourier-transform technique. A least-squares, cross-spectral analysis (Geometrics, 2000) is then used to solve for a transfer function (impedance) that relates the observed electric fields to the magnetic fields under the assumption that the earth consists of a two-input, two-output, linear system with the magnetic fields as input and the electric fields as output.

For a two-dimensional (2-D) earth, the diagonal terms of the impedance tensor are zero. The off-diagonal terms are decoupled into transverse electric (TE) and transverse magnetic (TM) modes. When the geology satisfies the 2-D assumption, the MT and AMT data for the TE mode measures electric field parallel to geologic strike, and the data for the TM mode measures electric field perpendicular to geologic strike. Data are processed with a fixed rotation parallel and perpendicular to regional strike. The MT and AMT methods are well suited for studying complicated geological environments because the electric and magnetic relations are sensitive to vertical and horizontal variations in resistivity. The method is capable of establishing whether the EM fields are responding to subsurface terranes of 1-, 2-, or 3-dimensions. For more information on this technique, see Telford and others (1991) for an introduction to the MT method and Vozoff (1991) for a more advanced treatment.

Audiomagnetotelluric Survey

AMT sounding data were acquired along four profile lines in eastern Nevada (Figure 1). A description of each line is given in Table 1. In addition to these profiles, a fifth transect, Profile D, was attempted in Coyote Spring Valley (Figure 1). However, this line was aborted due to the distortion of the data from nearby power lines, and the data are not presented here. Access to all but a few stations was with a truck along dirt roads. All soundings were collected with a Geometrics StrataGem EH-4 system (Geometrics, 2000). Horizontal electric fields were measured using Model BE-26 Buffered Active High Frequency dipoles and stainless steel electrodes in an X-shaped array with nominal dipole lengths of 40 m. The two, horizontal and orthogonal components of the magnetic field are measured in the same direction as the electric-field array with permalloy-cored

BF-10 induction coils. Data were acquired in two frequency bands: 92,000 to 800 Hz and 1000 to 10 Hz.

Through experimentation we found that the optimal transmitter distance, at which the measurement site is located in the transmitter's far field and yet receives adequate signal power, was 200 to 300 m from the receiver array, and we were able to acquire two stations for each transmitter location.

Table 2 shows the AMT station locations and elevations for lines A, B, C, and E. Locations and elevations were recorded using a Garmin global positioning system during field acquisition.

Audiomagnetotelluric Data

After transforming the recorded time-series data to the frequency domain, standard processing (Geometrics, 2000) was employed to determine apparent resistivity and phase tensor at each site. Apparent resistivity is the ratio of one component of the electric field magnitude over the orthogonal component of the magnetic field magnitude, normalized by the frequency and the magnetic susceptibility for free space. The impedance phase is the arctangent of the unnormalized ratio. The apparent resistivity and phase are related through a Hilbert transform; the phase is proportional to the slope of the apparent resistivity curve on a log-log plot, but from a baseline of 45 degrees (Vozoff, 1991).

Predicted values of the electric field can be computed from the measured values of the magnetic field (Vozoff, 1991). The coherence of the predicted electric field with the measured electric field is a measure of the signal-to-noise ratio provided in the E-predicted coherency plots.

Values are normalized between 0 and 1, where values at 0.5 signify signal levels equal to noise levels.

Anthropomorphic noise, such as power lines, power generators, moving vehicles and trains, can produce an incoherent noise mainly affecting frequencies above 1 Hz. An ungrounded, barbed wire fence along Profile A did not influence the data. Noise sources were absent from Profiles B and E. Data along Profile C were noisier than the other profiles: A power line located over 10 km away from Profile C was the only known source of noise in the area, and we do not have explanations for the increased broadband noise on several soundings.

Several soundings were recorded at each station. The best sounding from each station is presented here and will be used in subsequent modeling of the data. The unedited data presented here are not rotated, but fixed at specific azimuths as acquired in the field (Table 1). The ExHy mode is the nominal TM and the EyHx the TE mode. Scalar data as calculated in the Imagem presentational software (Geometrics, 2000) are presented. For each station, three separate plots are given in Appendix A:

1. Apparent Resistivity for the TM and TE modes at a fixed direction.
2. Impedance Phase for the TM and TE modes at a fixed direction.
3. E-Predicted Coherencies are $(ExHy * Conj(ExHy)) / (Hy * Conj(Hy) * Ex * Conj(Ex))$ and $(EyHx * Conj(EyHx)) / (Hx * Conj(Hx) * Ey * Conj(Ey))$, where Conj indicates complex conjugation.

Electronic data are available upon request in two formats: Geometrics Z Impedance files (Geometrics, 2000; Appendix A) and the Electronic Data Interchange (EDI), which was established in 1987 by the Society of Exploration Geophysicists (SEG) as a standard format for the interchange of MT data (Wright, 1988).

Acknowledgments

This study was performed in cooperation with the Southern Nevada Water Authority (SNWA) whose support is greatly appreciated. We are grateful to Janet Tilden for her help in the field, and to Gary Dixon, Jeff Johnston, and Ester Falgás Parra for contributing their expertise and advice. We also thank Ed Mankinen and Vicki Langenheim for their helpful reviews.

References Cited

- Eberhart-Phillips, D., Stanley, W.D., Rodriguez, B.D. and Lutter, W.J., 1995, Surface seismic and electrical methods to detect fluids related to faulting: *Journal of Geophysical Research*, vol. 100, no. B7, p. 12,919-12,936.
- Geometrics, 2000, Operation Manual for Stratagem systems running IMAGEM, Ver. 2.16: Geometrics, San Jose, California.
- Harrill, J.R., and Prudic, D.E., 1998, Aquifer systems in the Great Basin region of Nevada, Utah and adjacent states – summary report: U.S. Geological Professional Paper, 1409A, 61p.
- Keller, G.V., 1987, Rock and mineral properties, *in* *Electromagnetic Methods in Applied Geophysics Theory*: M.N. Nabighian, Ed., Society of Exploration Geophysicists, Tulsa, Oklahoma, v.1, p. 13-51.
- Keller, G.V., 1989, Electrical properties, *in* Carmichael, R.S., Ed., *Practical handbook of physical properties of rocks and minerals*: CRC Press, Boca Raton, Florida, p. 359-427.
- Mankinen, E.A., Roberts, C.W., McKee, E.H., Chuchel, B.A., and Moring, B.C., 2006, Geophysical data from the Spring and Snake valleys area, Nevada and Utah: U.S. Geological Survey Open-File Report 2006-1160, 42 p.

- Palacky, G.J., 1987, Resistivity characteristics of geologic targets, *in* *Electromagnetic Methods in Applied Geophysics Theory*: M.N. Nabighian, Ed., Society of Exploration Geophysicists, Tulsa, Oklahoma, vol. 1, p. 53-129.
- Scheirer, D.S., 2005, Gravity studies of Cave, Dry Lake, and Delamar Valleys, east-central Nevada: U.S. Geological Survey Open File Report, 2005-1339, 36p.
- Telford, W.M., Geldart, L.P., and Sheriff, R.E., 1991, *Applied Geophysics* (2nd Edition): Cambridge University Press, 790 p.
- Vozoff, K., 1991, The magnetotelluric method, *in* *Electromagnetic methods in applied geophysics*: M.N. Nabighian, Ed., Society of Exploration Geophysicists, Tulsa, Oklahoma, vol. 2, part B, p. 641-711.
- Wright, D.E., 1988, The SEG Standard for Magnetotelluric Data: presented at the Society of Exploration Geophysicists Annual Meeting, November. Available through <http://www.geophysics.dias.ie/mtnet/docs/ediformat.txt>.
- Zonge, K.L. and Hughes, L.J., 1991, Controlled source audio-frequency magnetotellurics, *in* *Electromagnetic methods in applied geophysics*: M.N. Nabighian, Ed., Society of Exploration Geophysicists, Tulsa, Oklahoma, vol. 2, part B, p. 713-809.

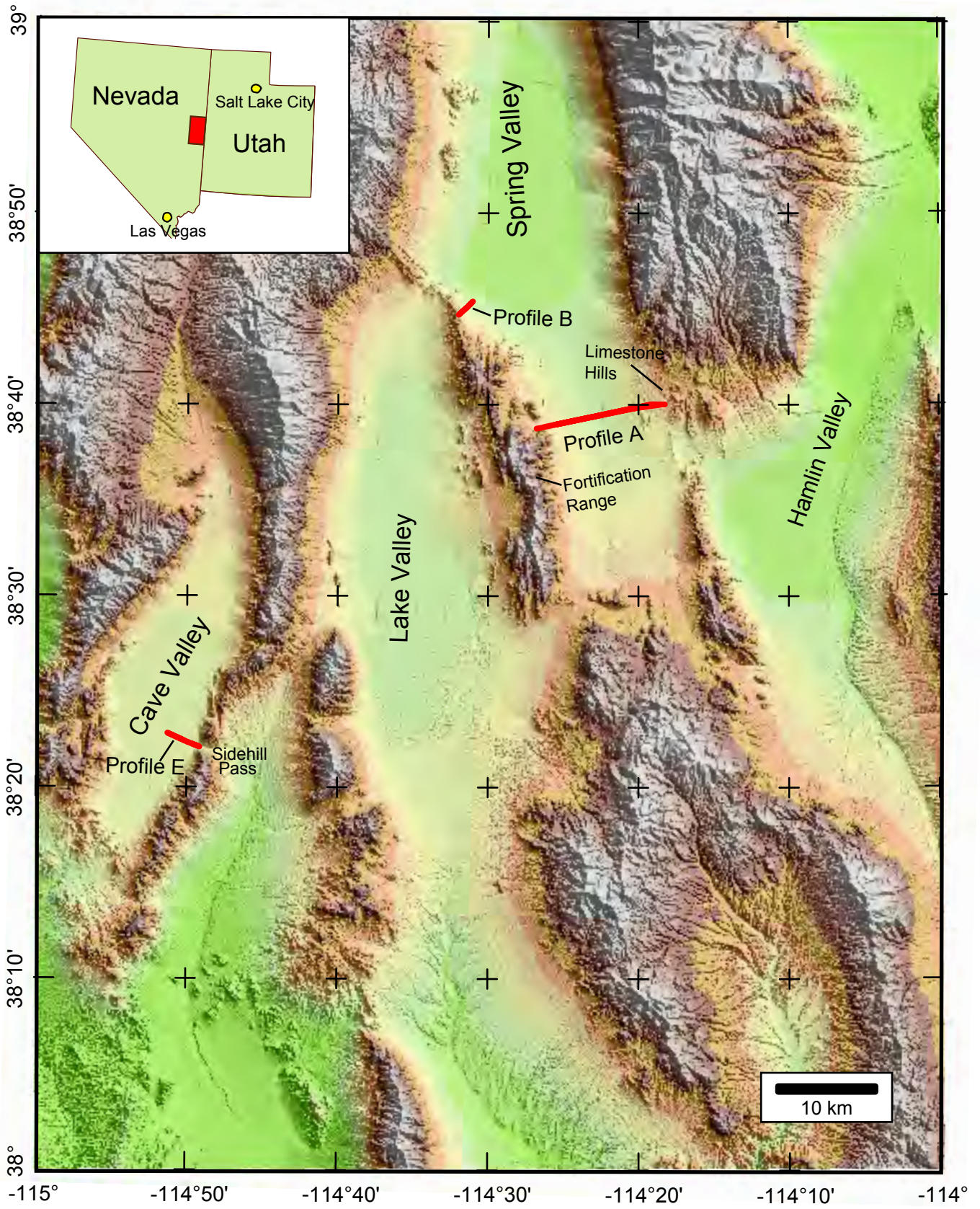


Figure 1A. Topographic map of study area showing location of profiles A,B, and E.

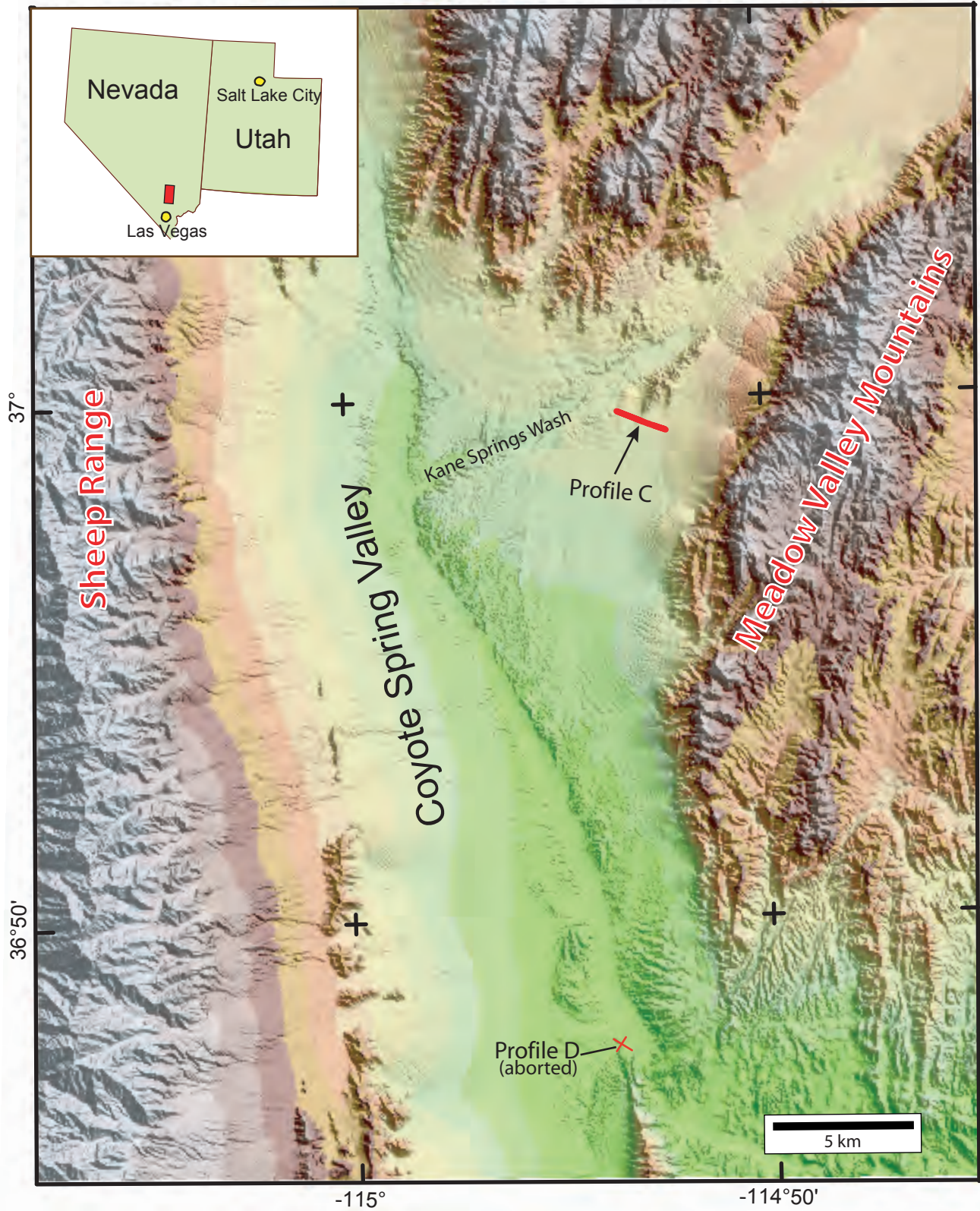


Figure 1B. Topographic map of study area showing location of profile C.

Table 1. Description of AMT profiles.

[Azimuth refers to the magnetic orientation of the x-direction, which remained fixed throughout each profile]

Profile	Length	Azimuth (x-direction)	Station Spacing	Number of Stations	Comments
A	12.6 km	80°	200m	64	Across southern Spring Valley from the Fortification Range (west) to the Limestone Hills (east).
B	2.2 km	80°	200-400m	9	North of Fortification Range, west side of Spring Valley
C	1.4 km	100°	100-200m	9	Eastern Coyote Spring Valley near Kane Springs Wash
D	N/A	N/A	N/A	N/A	Aborted due to power line interference
E	3.0 km	100°	200-400m	14	Cave Valley west of Sidehill Pass

Table 2. Sounding numbers, locations and elevations of stations along four AMT profiles.

[Distance indicates distance along profile in meters, where positive is east. Latitude and longitude are in NAD 27 decimal degrees. Universal Transverse Mercator (zone 11N) units are in meters. Horizontal locations are accurate to approximately 3 m (10 ft.) Station elevation is given in meters and feet and are accurate to approximately 7 m (23 ft.).]

Profile A (SVNA)							
Sounding	Distance (m)	Latitude	Longitude	Easting (m)	Northing (m)	Elevation (m)	Elevation (ft)
4	0	38.6459	-114.4465	722154	4280566	1898	6228
5	200	38.6463	-114.4440	722368	4280617	1891	6204
6	400	38.6465	-114.4420	722542	4280652	1888	6193
7	600	38.6469	-114.4398	722737	4280694	1884	6180
8	800	38.6474	-114.4375	722931	4280755	1880	6169
10	1000	38.6477	-114.4353	723126	4280799	1868	6128
12	1200	38.6481	-114.4330	723320	4280846	1878	6161
15	1400	38.6484	-114.4307	723519	4280891	1858	6097
17	1600	38.6488	-114.4285	723713	4280933	1847	6060
54	1800	38.6492	-114.4263	723902	4280990	1853	6078
18	2000	38.6496	-114.4240	724099	4281035	1848	6062
56	2200	38.6499	-114.4217	724296	4281078	1848	6063
19	2400	38.6503	-114.4195	724487	4281126	1839	6035

57	2600	38.6507	-114.4173	724682	4281178	1843	6045
20	2800	38.6511	-114.4150	724878	4281225	1836	6024
58	3000	38.6515	-114.4128	725072	4281270	1836	6025
21	3200	38.6519	-114.4105	725269	4281319	1832	6009
59	3400	38.6523	-114.4083	725461	4281369	1831	6007
23	3600	38.6526	-114.4060	725661	4281412	1825	5988
60	3800	38.6530	-114.4037	725856	4281457	1826	5992
24	4000	38.6533	-114.4015	726047	4281502	1818	5964
61	4200	38.6537	-114.3992	726243	4281550	1820	5970
25	4400	38.6541	-114.3970	726434	4281600	1811	5943
62	4600	38.6545	-114.3948	726630	4281647	1812	5944
26	4800	38.6548	-114.3925	726823	4281692	1799	5902
63	5000	38.6552	-114.3903	727017	4281742	1810	5937
28	5200	38.6556	-114.3880	727216	4281791	1806	5924
64	5400	38.6560	-114.3858	727405	4281836	1812	5946
30	5600	38.6562	-114.3835	727606	4281864	1805	5922
65	5800	38.6567	-114.3813	727795	4281932	1802	5911
32	6000	38.6571	-114.3790	727990	4281976	1823	5980
67	6200	38.6574	-114.3768	728187	4282020	1803	5915
34	6400	38.6579	-114.3745	728380	4282074	1803	5915
68	6600	38.6582	-114.3722	728578	4282117	1816	5959
35	6800	38.6586	-114.3700	728770	4282168	1815	5955
69	7000	38.6590	-114.3678	728963	4282213	1812	5946
95	7200	38.6593	-114.3655	729159	4282260	1828	5997
70	7400	38.6597	-114.3633	729350	4282309	1819	5967
39	7600	38.6601	-114.3610	729550	4282358	1826	5992
71	7800	38.6605	-114.3588	729742	4282403	1830	6005
40	8000	38.6608	-114.3565	729935	4282450	1832	6010
72	8200	38.6612	-114.3543	730133	4282494	1832	6012
41	8400	38.6616	-114.3520	730327	4282545	1834	6016
74	8600	38.6620	-114.3498	730520	4282593	1837	6028
43	8800	38.6623	-114.3475	730717	4282638	1843	6045
75	9000	38.6627	-114.3453	730909	4282685	1848	6062
45	9200	38.6631	-114.3430	731105	4282731	1853	6078
77	9400	38.6635	-114.3408	731297	4282781	1855	6086
46	9600	38.6638	-114.3385	731493	4282820	1860	6104
78	9800	38.6642	-114.3363	731688	4282872	1866	6121
47	10000	38.6646	-114.3336	731923	4282930	1872	6142
80	10200	38.6649	-114.3318	732076	4282965	1875	6152
49	10400	38.6653	-114.3295	732273	4283012	1878	6162
82	10600	38.6657	-114.3273	732468	4283059	1884	6180
51	10800	38.6660	-114.3250	732663	4283107	1888	6195
83	11000	38.6664	-114.3228	732858	4283151	1895	6218
52	11200	38.6668	-114.3205	733055	4283201	1896	6219
84	11400	38.6671	-114.3182	733254	4283242	1904	6247
98	11600	38.6671	-114.3158	733458	4283245	1913	6277
87	11800	38.6671	-114.3135	733663	4283248	1915	6282
94	12000	38.6686	-114.3121	733857	4283221	1959	6246

88	12200	38.6671	-114.3090	734054	4283260	1914	6279
93	12400	38.6670	-114.3067	734255	4283259	1929	6329
102	12600	38.6670	-114.3040	734489	4283264	1911	6270
Profile B (SVNB)							
Sounding	Distance (m)	Latitude	Longitude	Easting (m)	Northing (m)	Elevation (m)	Elevation (ft)
107	-200	38.7644	-114.5394	713791	4293294	1805	5922
103	0	38.7654	-114.5375	713952	4293411	1789	5871
108	200	38.7664	-114.5356	714114	4293527	1790	5874
104	400	38.7672	-114.5335	714293	4293623	1783	5850
109	600	38.7677	-114.5314	714481	4293681	1770	5807
105	800	38.7677	-114.5280	714698	4293696	1769	5803
106	1200	38.7676	-114.5240	715118	4293691	1765	5792
111	1600	38.7674	-114.5195	715514	4293675	1764	5786
112	2000	38.7672	-114.5149	715911	4293665	1761	5777
Profile C (SVNC)							
Sounding	Distance (m)	Latitude	Longitude	Easting (m)	Northing (m)	Elevation (m)	Elevation (ft)
16	-600	36.9962	-114.8911	687590	4096521	871	2856
27	-400	36.9955	-114.8890	687778	4096450	876	2873
19	-200	36.9947	-114.8869	687965	4096365	875	2870
21	0	36.9944	-114.8847	688165	4096333	863	2831
33	100	36.9937	-114.8842	688212	4096264	871	2857
32	200	36.9933	-114.8830	688314	4096217	887	2911
23	400	36.9920	-114.8815	688456	4096075	888	2915
25	600	36.9918	-114.8791	688668	4096058	875	2870
30	800	36.9912	-114.8770	688854	4095993	882	2895
Profile E (SVNE)							
Sounding	Distance (m)	Latitude	Longitude	Easting (m)	Northing (m)	Elevation (m)	Elevation (ft)
16	-1800	38.3802	-114.8546	687319	4250168	1819	5972
14	-1400	38.3787	-114.8503	687698	4250011	1821	5979
13	-1000	38.3772	-114.8462	688063	4249858	1820	5976
12	-800	38.3765	-114.8441	688243	4249782	1823	5986
10	-600	38.3758	-114.8421	688426	4249711	1835	6024
7	-400	38.3750	-114.8400	688612	4249628	1820	5976
41	-200	38.3743	-114.8378	688799	4249554	1825	5991
4	0	38.3734	-114.8358	688978	4249459	1820	5974
39	200	38.3727	-114.8337	689163	4249385	1826	5996
19	400	38.3721	-114.8316	689352	4249319	1825	5990
23	600	38.3714	-114.8295	689539	4249249	1821	5978
36	800	38.3708	-114.8273	689729	4249180	1822	5982
26	1000	38.3701	-114.8253	689910	4249110	1828	6002
27	1200	38.3694	-114.8231	690100	4249042	1834	6022

Appendix

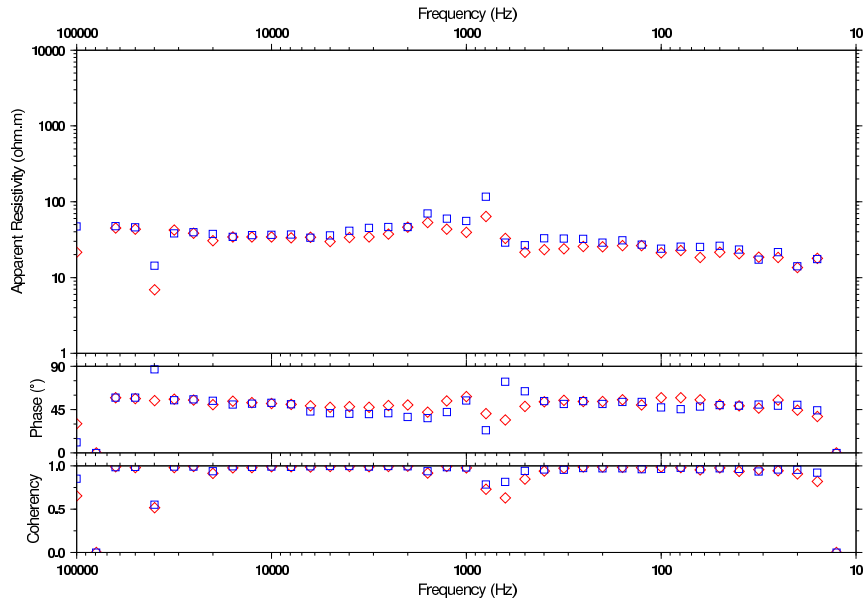
A. Sounding curves

The “Audiomagnetotelluric Data” section in this report contains an explanation for three separate plots for each station:

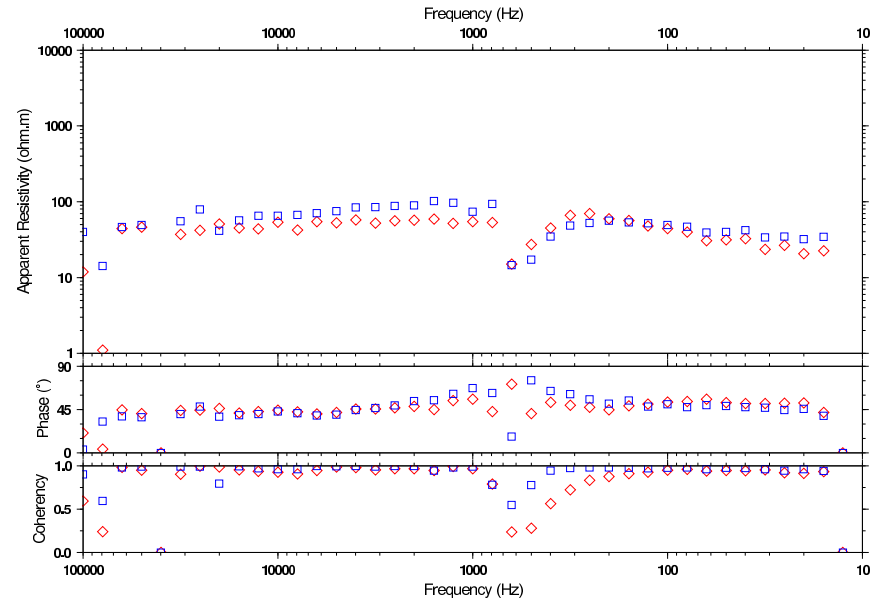
1. Apparent Resistivity for x-directed profile line such that the nominal TM mode is $E_x H_y$ (red diamond) and TE is $E_y H_x$ (blue square).
2. Impedance Phase for x-directed profile line such that the nominal TM mode is $E_x H_y$ (red diamond) and TE is $E_y H_x$ (blue square).
3. Multiple E-Predicted Coherencies, defined as $(E_x H_y * \text{Conj}(E_x H_y)) / (H_y * \text{Conj}(H_y) * E_x * \text{Conj}(E_x))$ (red diamond) and $(E_y H_x * \text{Conj}(E_y H_x)) / (H_x * \text{Conj}(H_x) * E_y * \text{Conj}(E_y))$ (blue square)

Sounding curves are named by profile name, distance along the profile (m) and sounding number, respectively. Note that for the distance along the profile, the positive direction trends eastward and the negative direction trends westward.

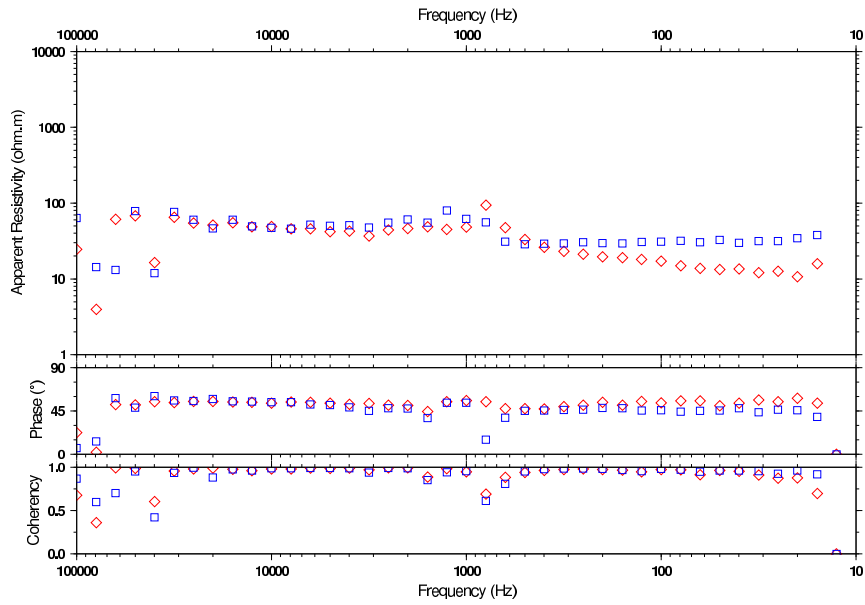
SVNA 00000m 004 - Scalar Res., Coherency, Phase (diamond=ExHy; square=EyHx)



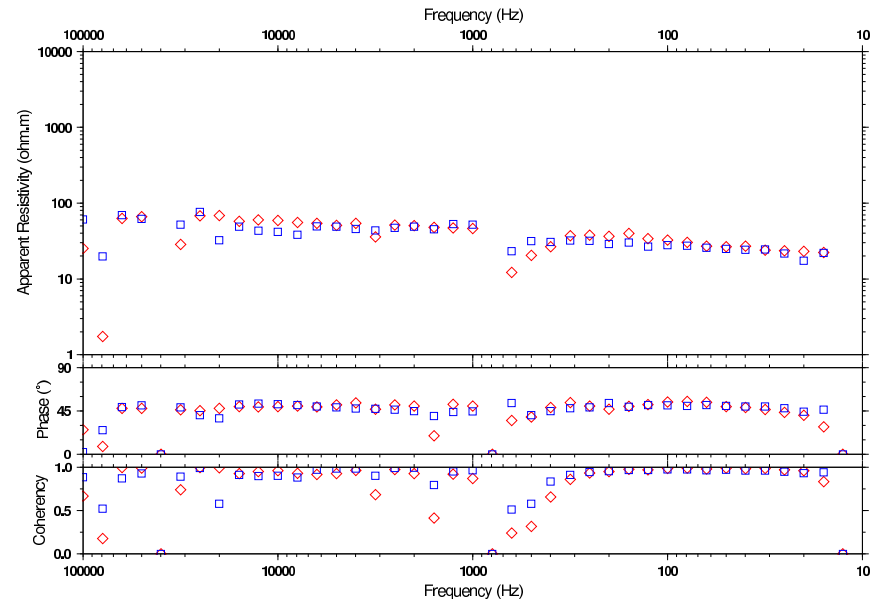
SVNA 00400m 006 - Scalar Res., Coherency, Phase (diamond=ExHy; square=EyHx)



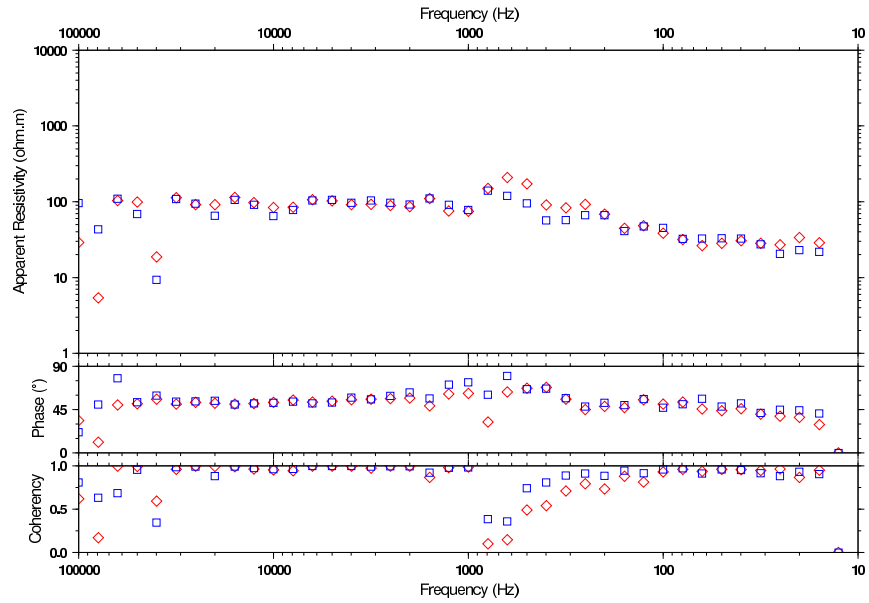
SVNA 00200m 005 - Scalar Res., Coherency, Phase (diamond=ExHy; square=EyHx)



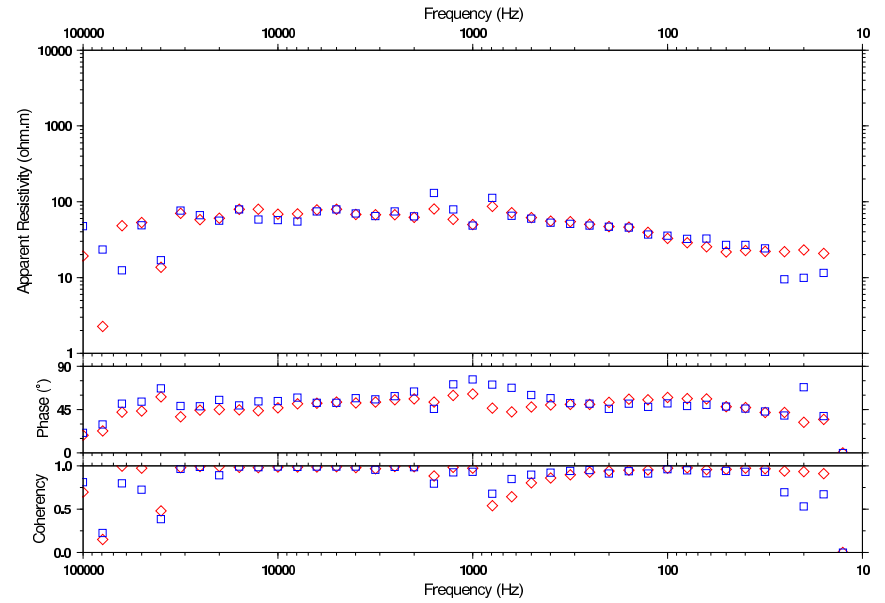
SVNA 00600m 007 - Scalar Res., Coherency, Phase (diamond=ExHy; square=EyHx)



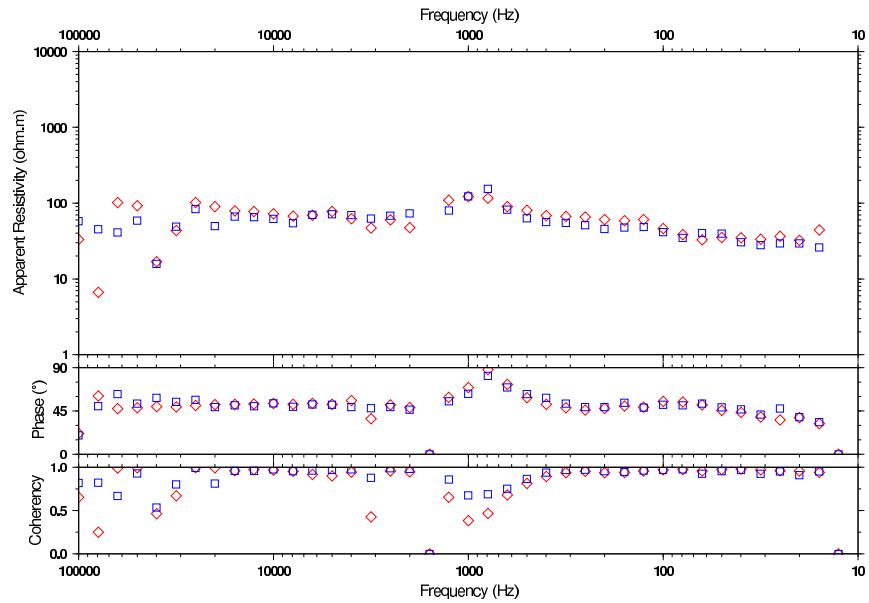
SVNA 00800m 008 - Scalar Res., Coherency, Phase (diamond=ExHy; square=EyHx)



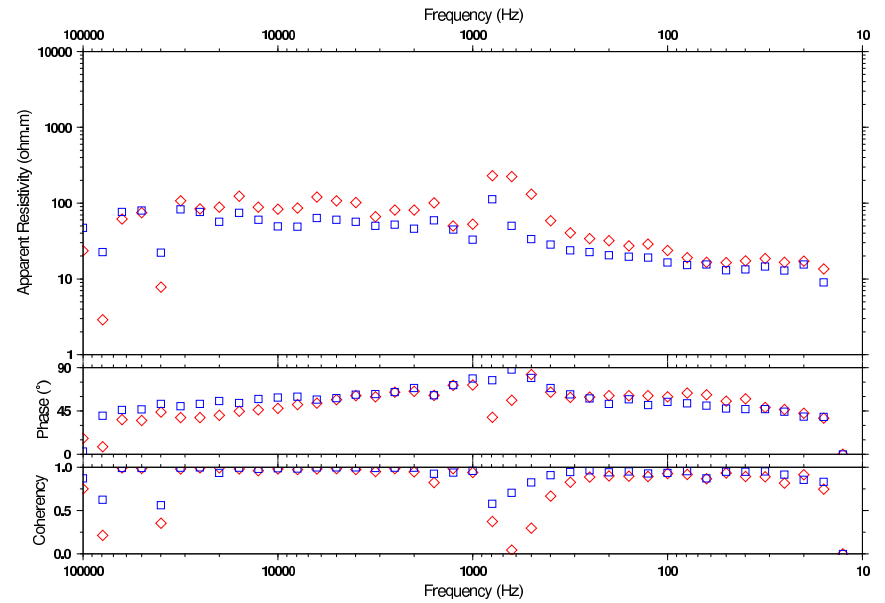
SVNA 01200m 012 - Scalar Res., Coherency, Phase (diamond=ExHy; square=EyHx)



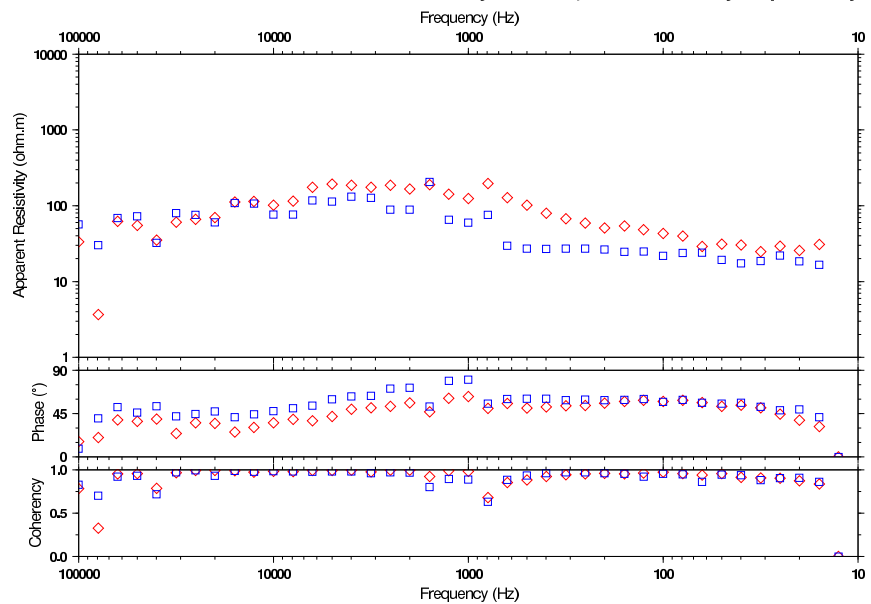
SVNA 01000m 010 - Scalar Res., Coherency, Phase (diamond=ExHy; square=EyHx)



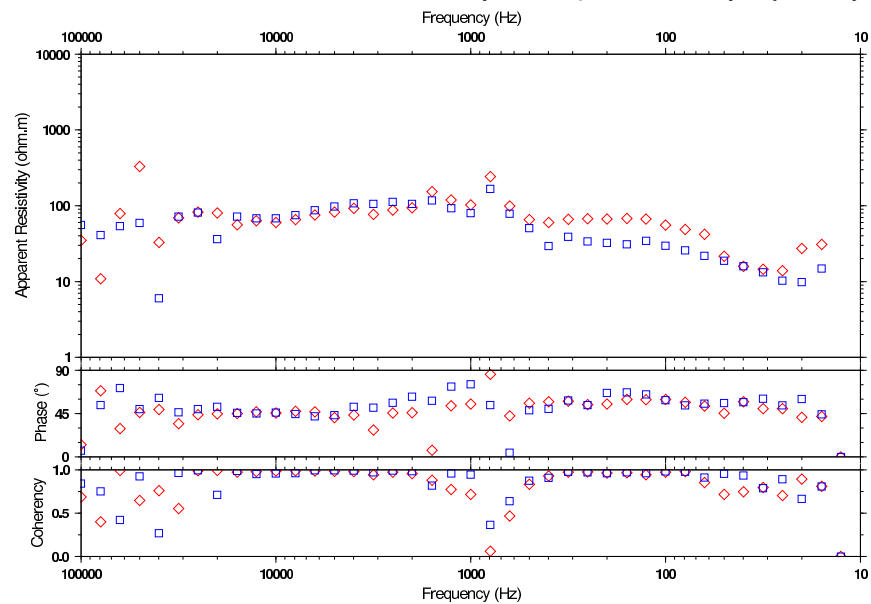
SVNA 01400m 015 - Scalar Res., Coherency, Phase (diamond=ExHy; square=EyHx)



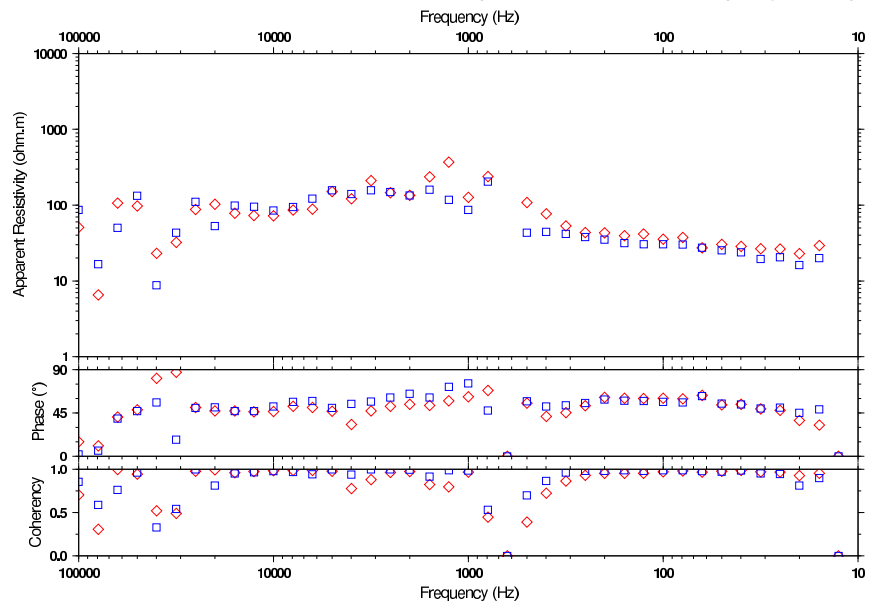
SVNA 01600m 017 - Scalar Res., Coherency, Phase (diamond=ExHy; square=EyHx)



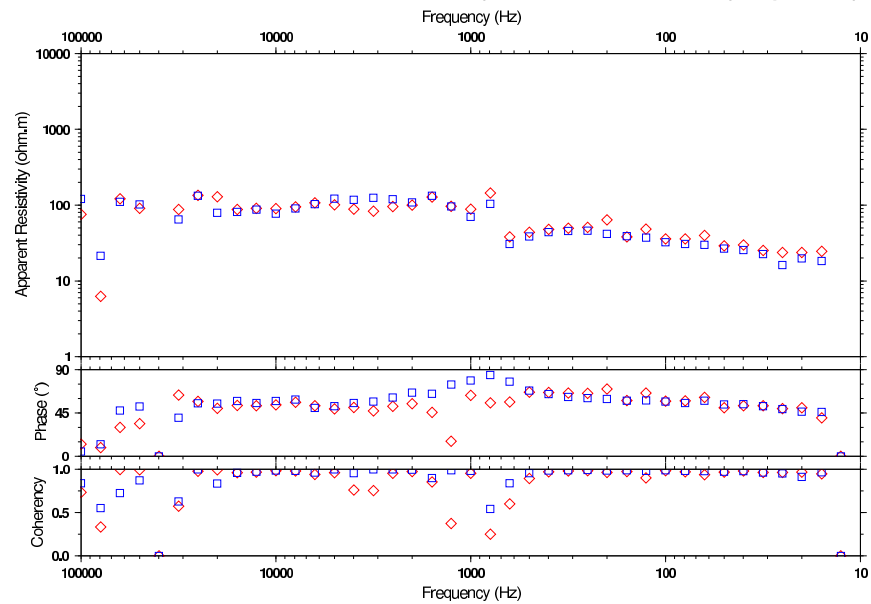
SVNA 02000m 018 - Scalar Res., Coherency, Phase (diamond=ExHy; square=EyHx)



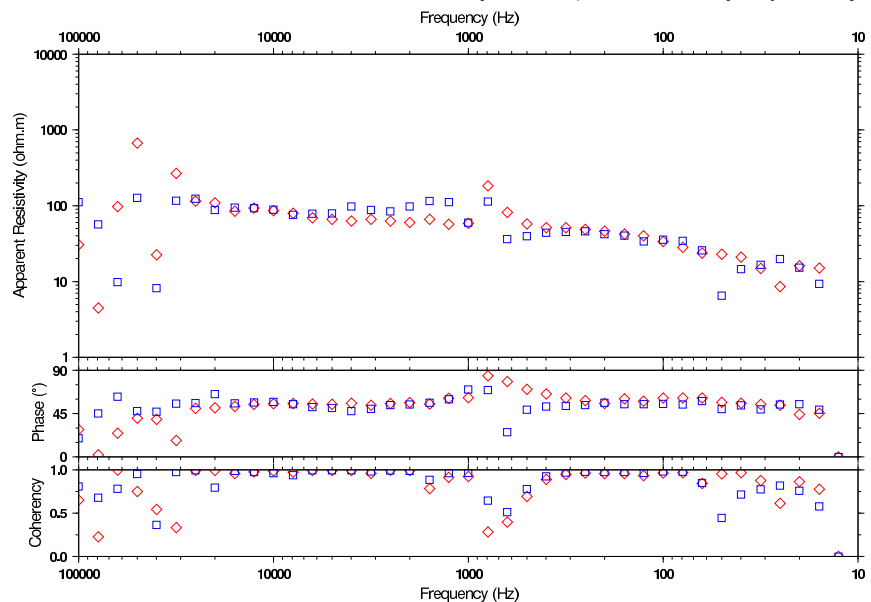
SVNA 01800m 054 - Scalar Res., Coherency, Phase (diamond=ExHy; square=EyHx)



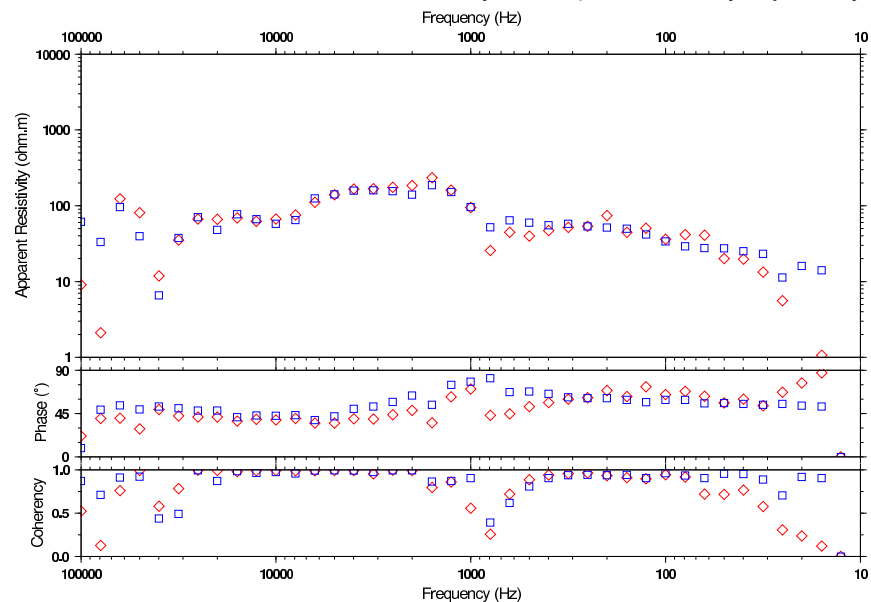
SVNA 02200m 056 - Scalar Res., Coherency, Phase (diamond=ExHy; square=EyHx)



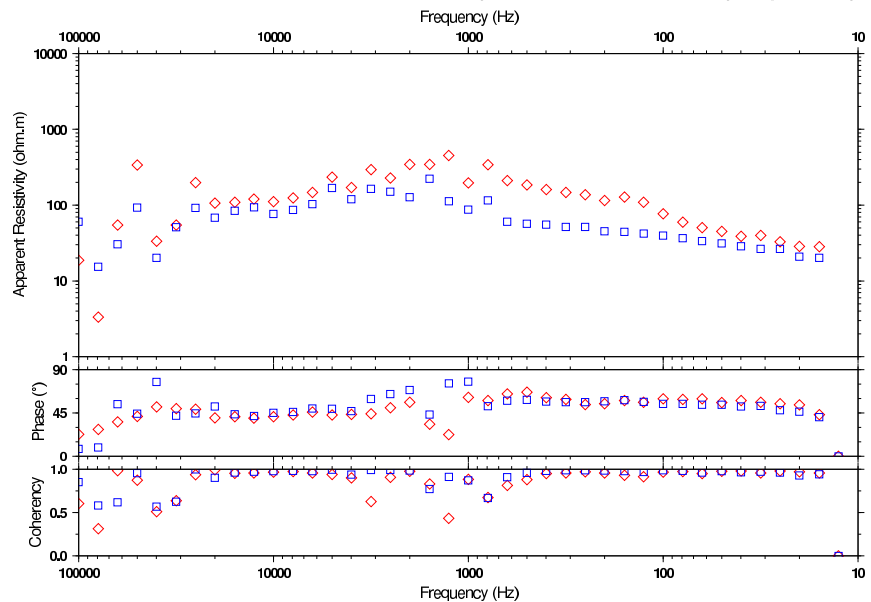
SVNA 02400m 019 - Scalar Res., Coherency, Phase (diamond=ExHy; square=EyHx)



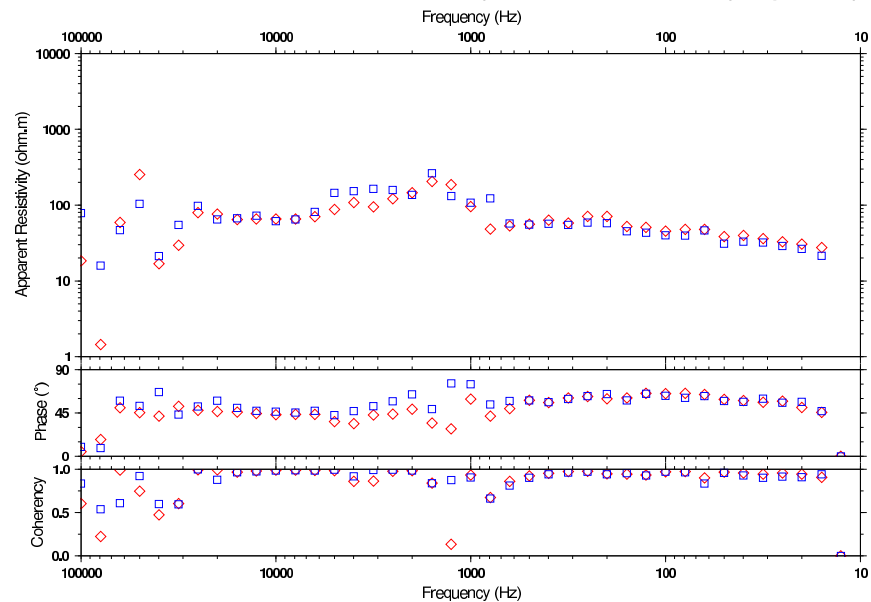
SVNA 02800m 020 - Scalar Res., Coherency, Phase (diamond=ExHy; square=EyHx)



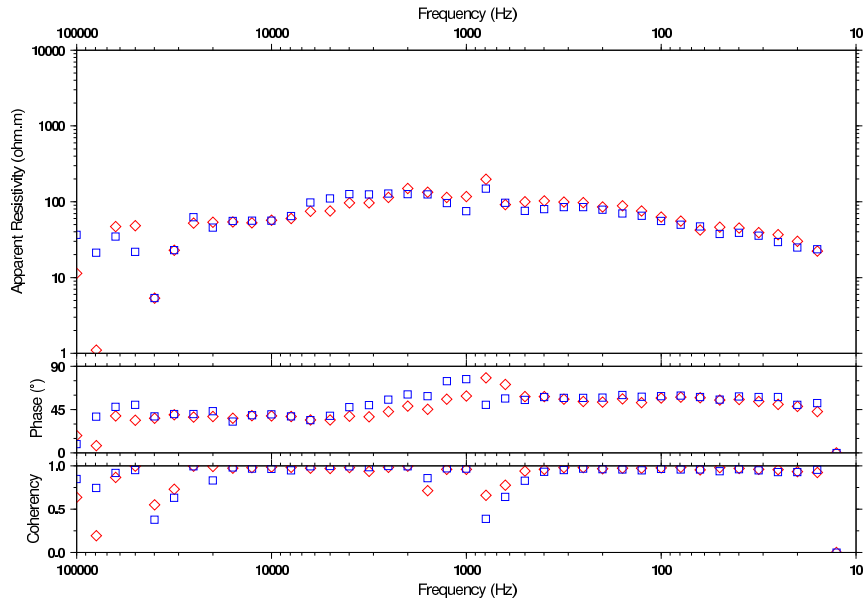
SVNA 02600m 057 - Scalar Res., Coherency, Phase (diamond=ExHy; square=EyHx)



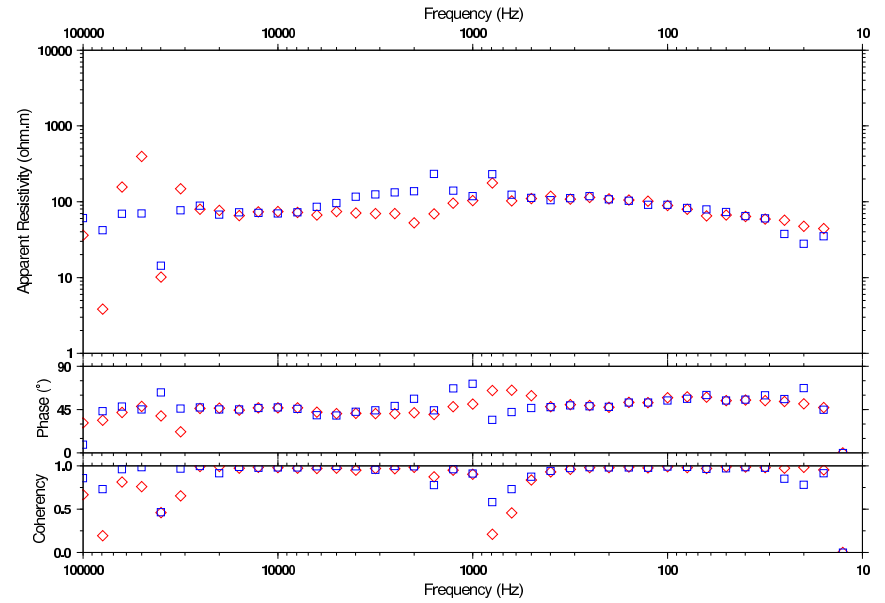
SVNA 03000m 058 - Scalar Res., Coherency, Phase (diamond=ExHy; square=EyHx)



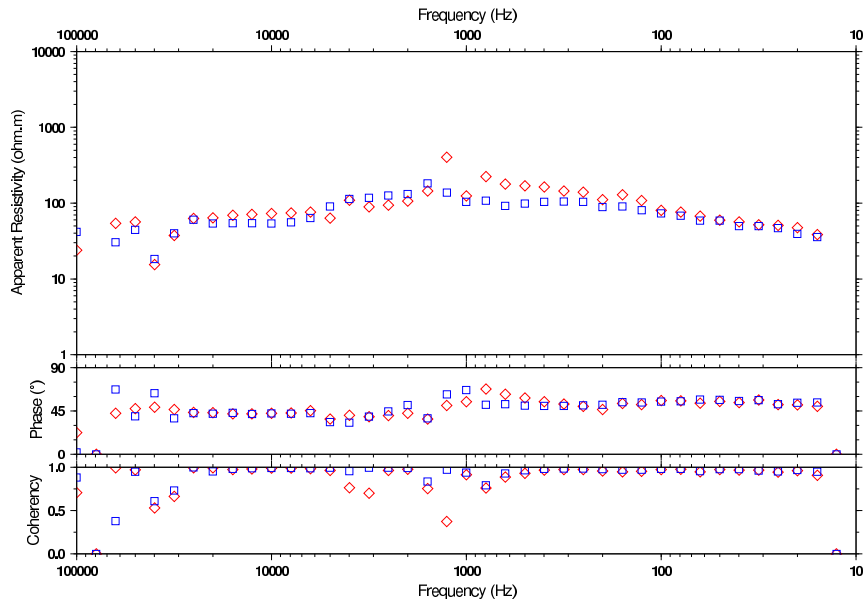
SVNA 03200m 021 - Scalar Res., Coherency, Phase (diamond=ExHy; square=EyHx)



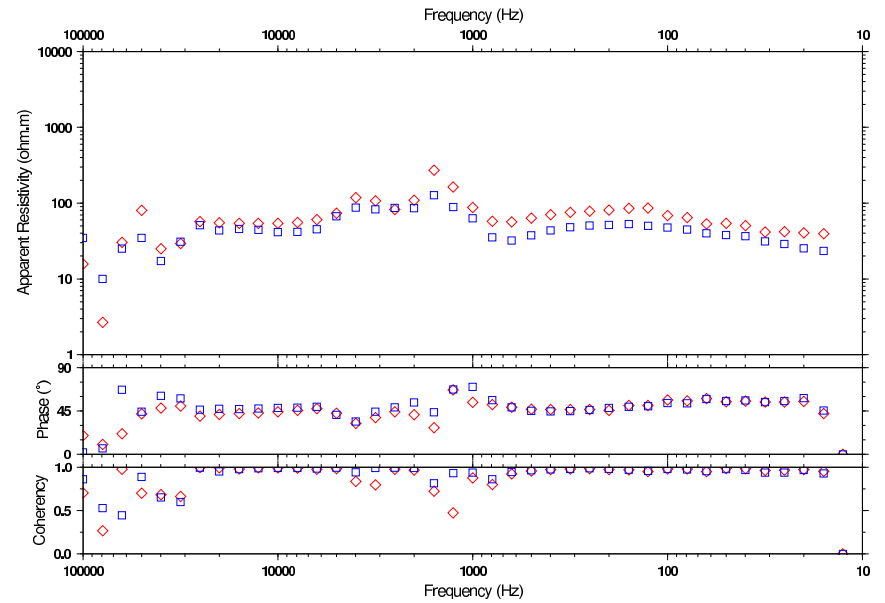
SVNA 03600m 023 - Scalar Res., Coherency, Phase (diamond=ExHy; square=EyHx)



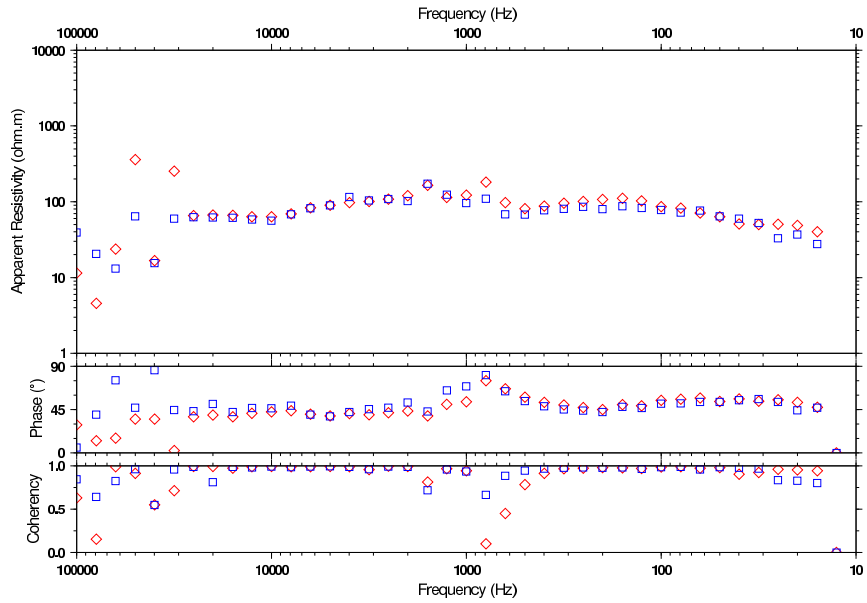
SVNA 03400m 059 - Scalar Res., Coherency, Phase (diamond=ExHy; square=EyHx)



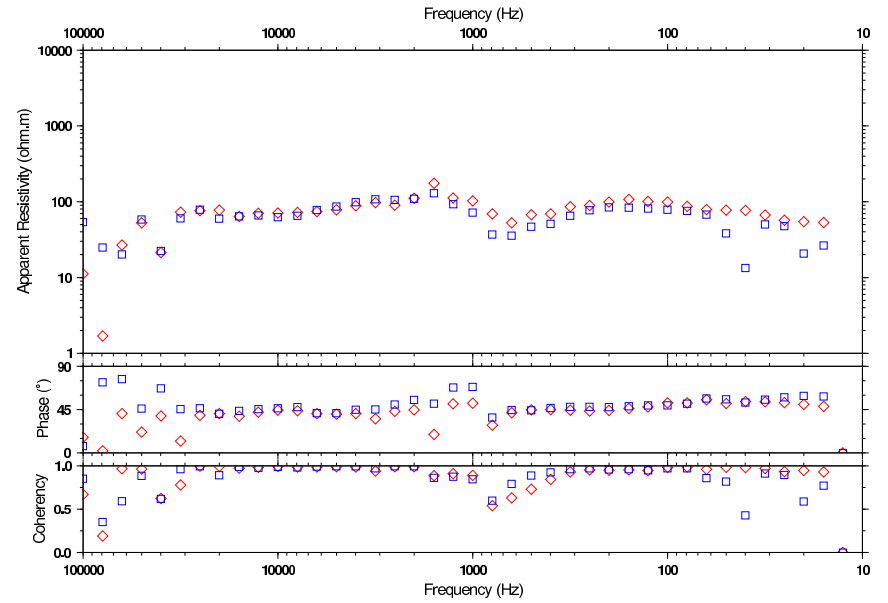
SVNA 03800m 060 - Scalar Res., Coherency, Phase (diamond=ExHy; square=EyHx)



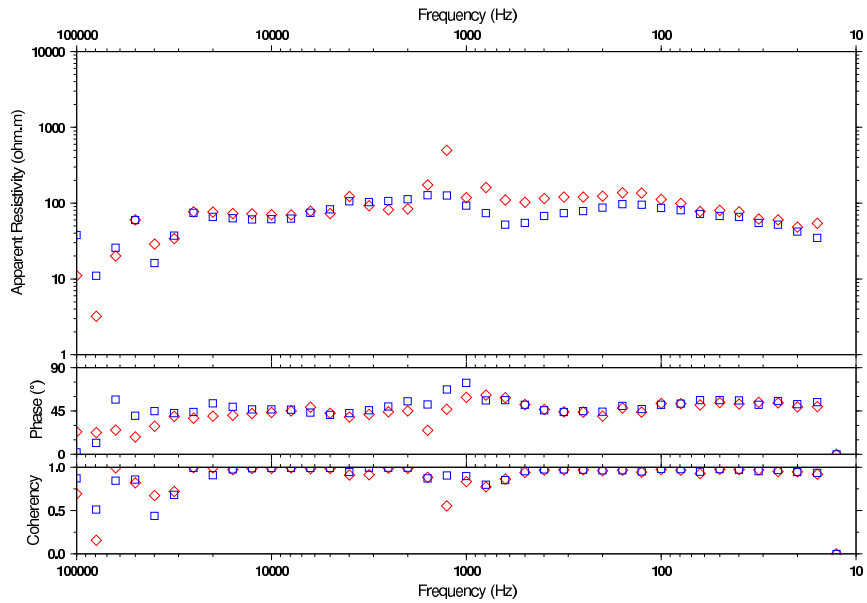
SVNA 04000m 024 - Scalar Res., Coherency, Phase (diamond=ExHy; square=EyHx)



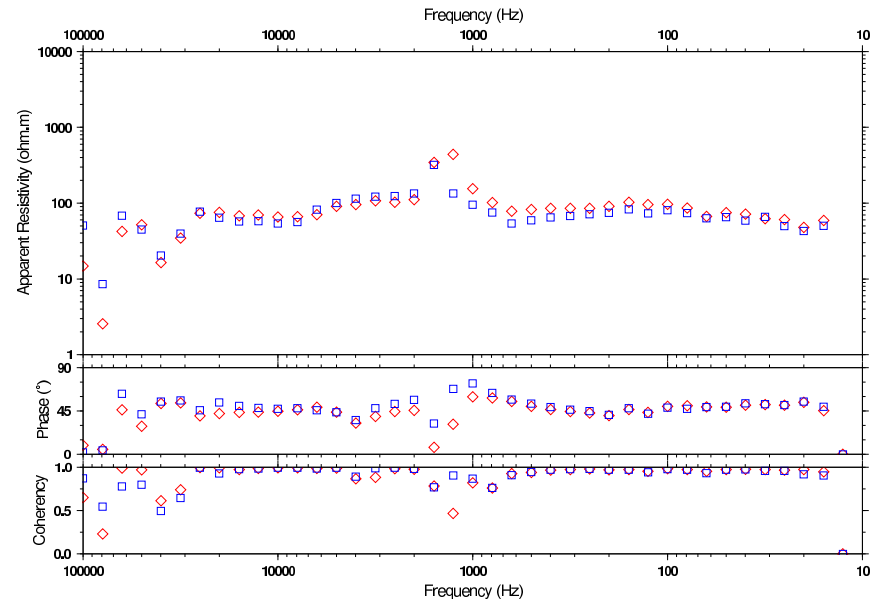
SVNA 04400m 025 - Scalar Res., Coherency, Phase (diamond=ExHy; square=EyHx)



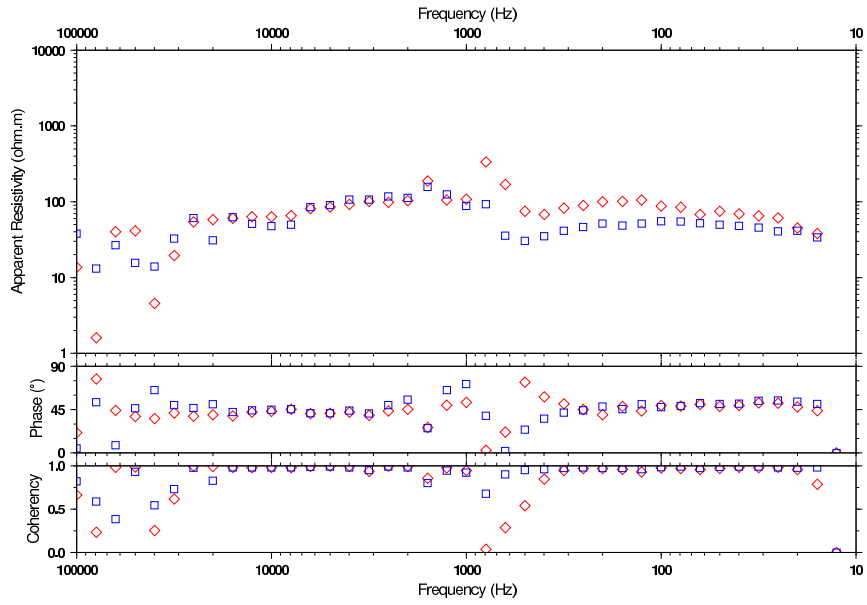
SVNA 04200m 061 - Scalar Res., Coherency, Phase (diamond=ExHy; square=EyHx)



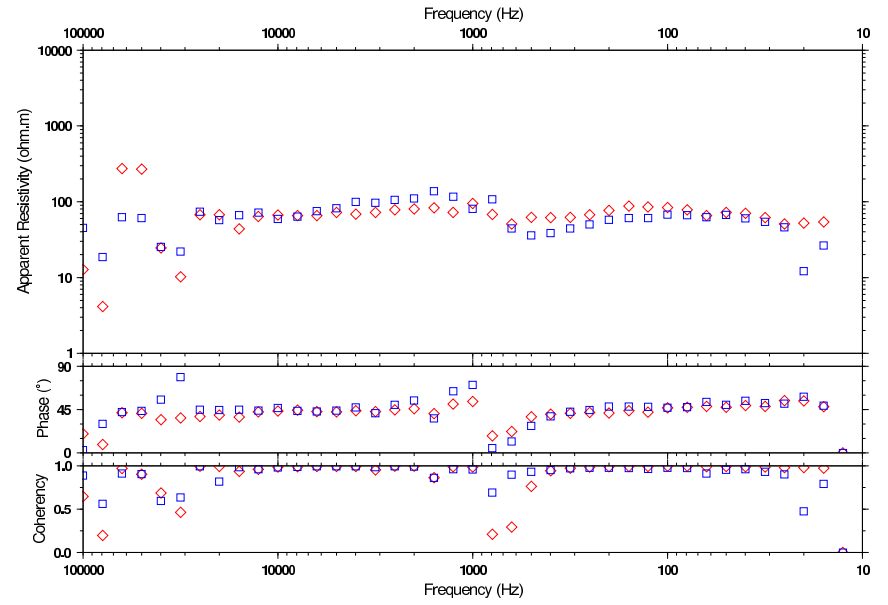
SVNA 04600m 062 - Scalar Res., Coherency, Phase (diamond=ExHy; square=EyHx)



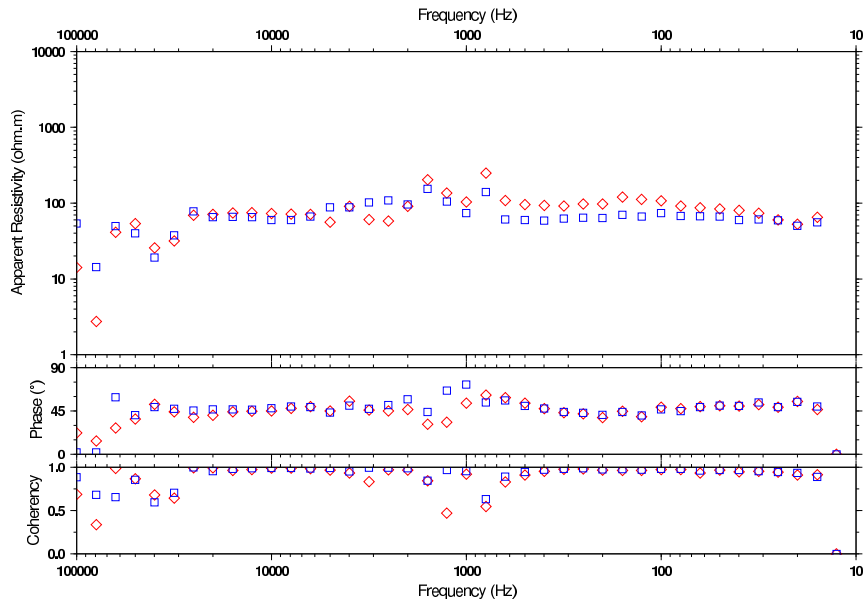
SVNA 04800m 026 - Scalar Res., Coherency, Phase (diamond=ExHy; square=EyHx)



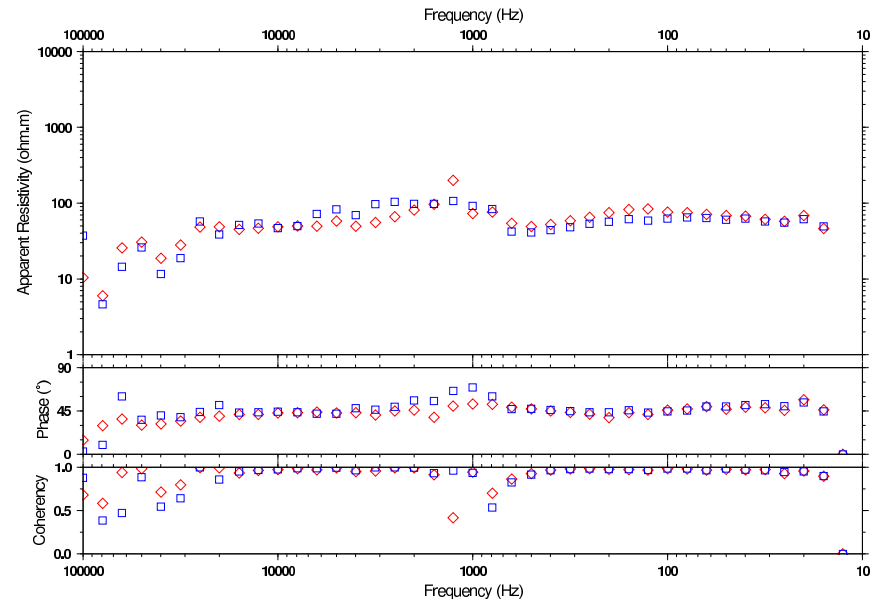
SVNA 05200m 028 - Scalar Res., Coherency, Phase (diamond=ExHy; square=EyHx)



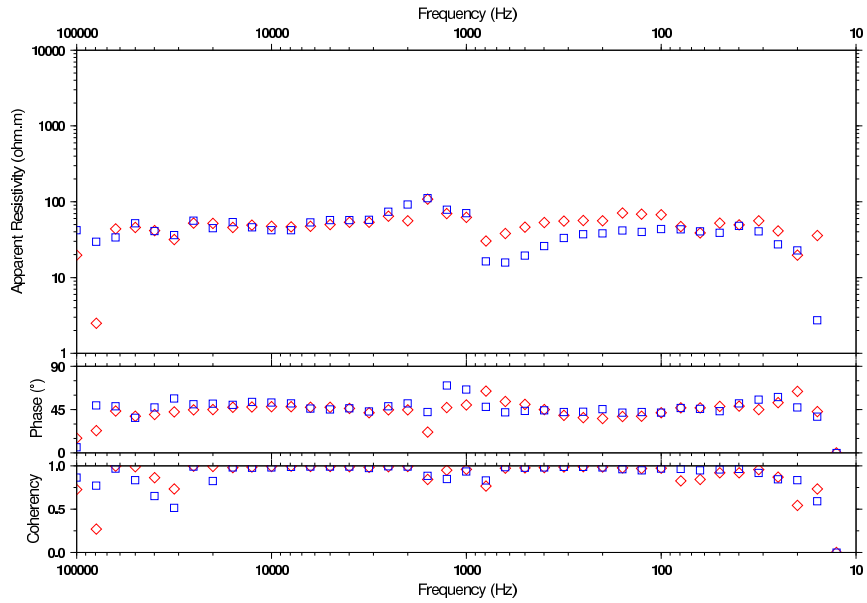
SVNA 05000m 063 - Scalar Res., Coherency, Phase (diamond=ExHy; square=EyHx)



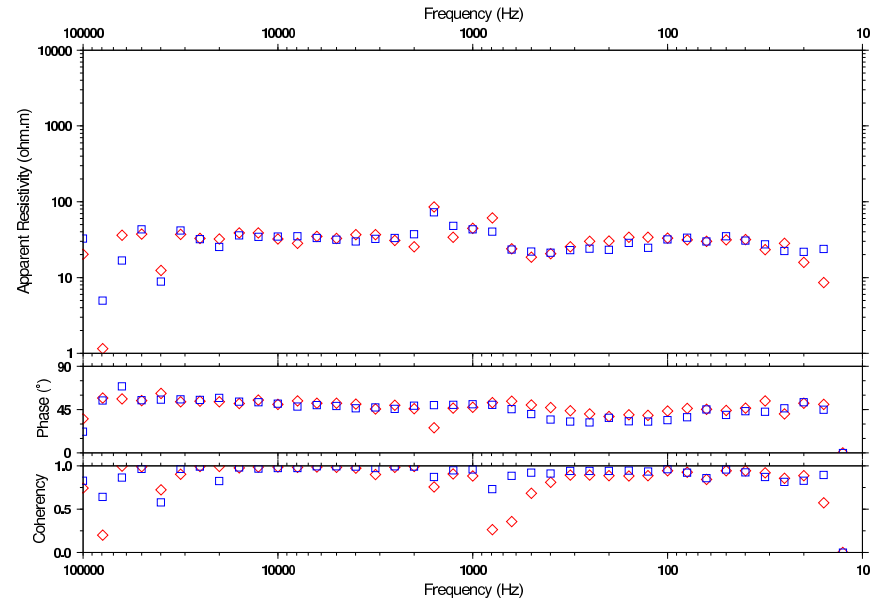
SVNA 05400m 064 - Scalar Res., Coherency, Phase (diamond=ExHy; square=EyHx)



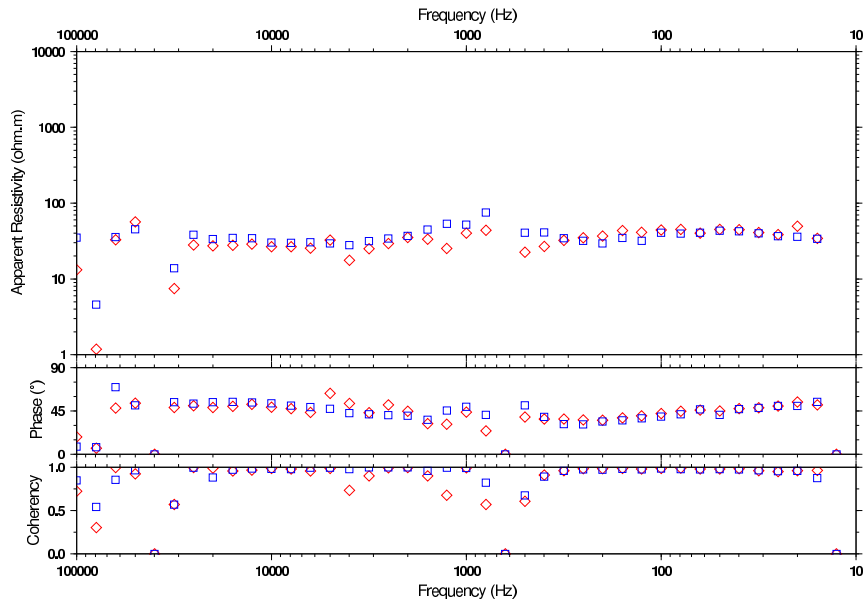
SVNA 05600m 030 - Scalar Res., Coherency, Phase (diamond=ExHy; square=EyHx)



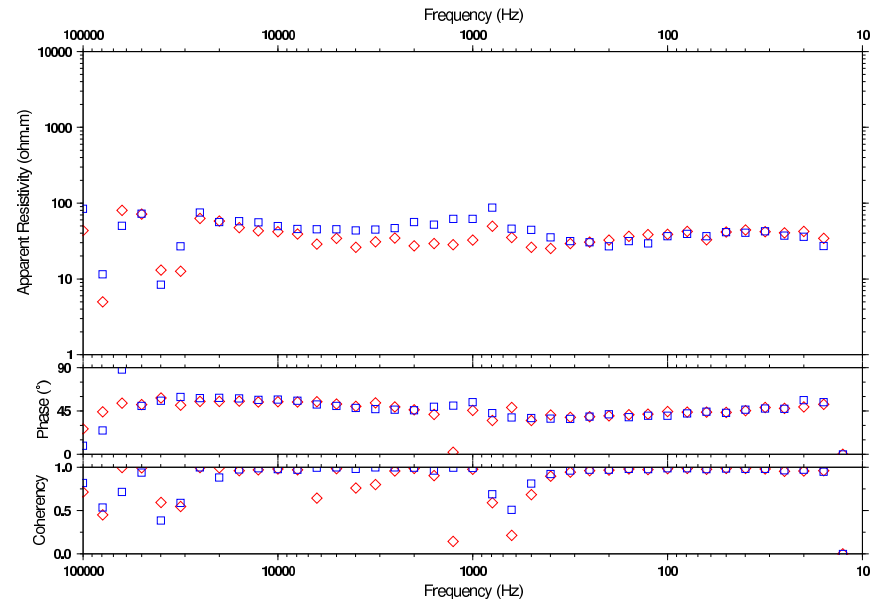
SVNA 06000m 032 - Scalar Res., Coherency, Phase (diamond=ExHy; square=EyHx)



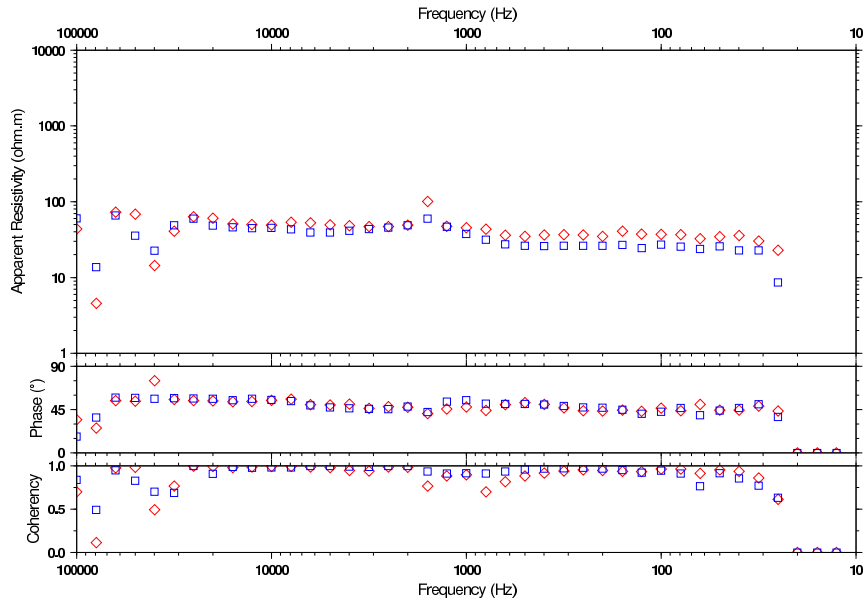
SVNA 05800m 065 - Scalar Res., Coherency, Phase (diamond=ExHy; square=EyHx)



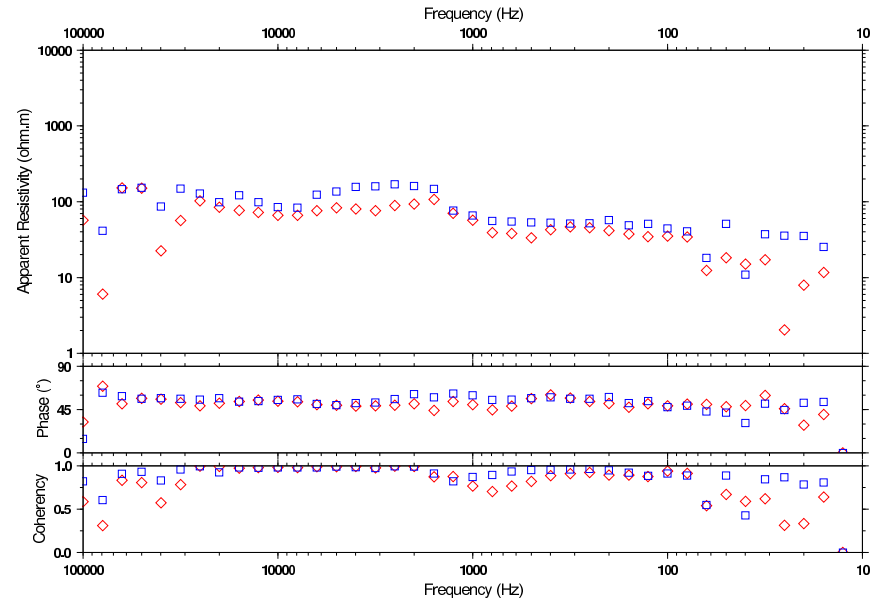
SVNA 06200m 067 - Scalar Res., Coherency, Phase (diamond=ExHy; square=EyHx)



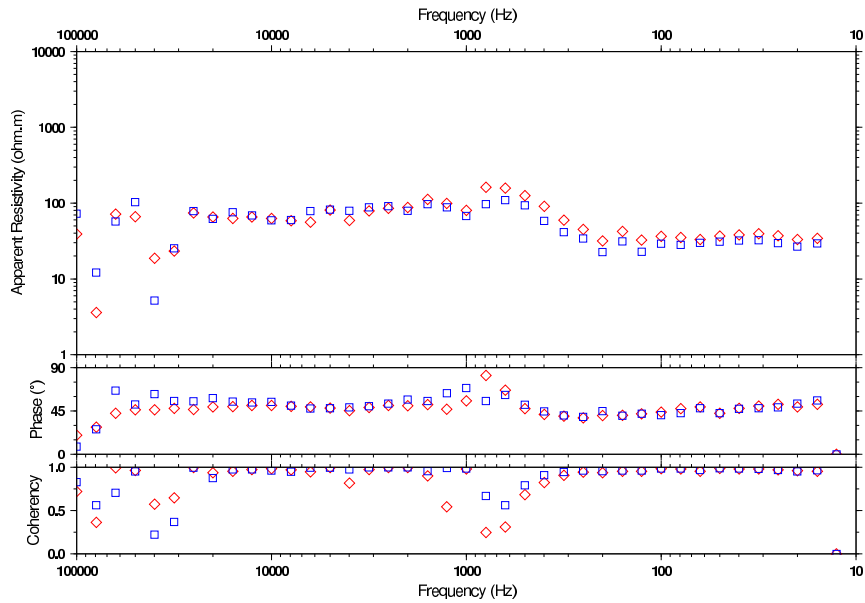
SVNA 06400m 034 - Scalar Res., Coherency, Phase (diamond=ExHy; square=EyHx)



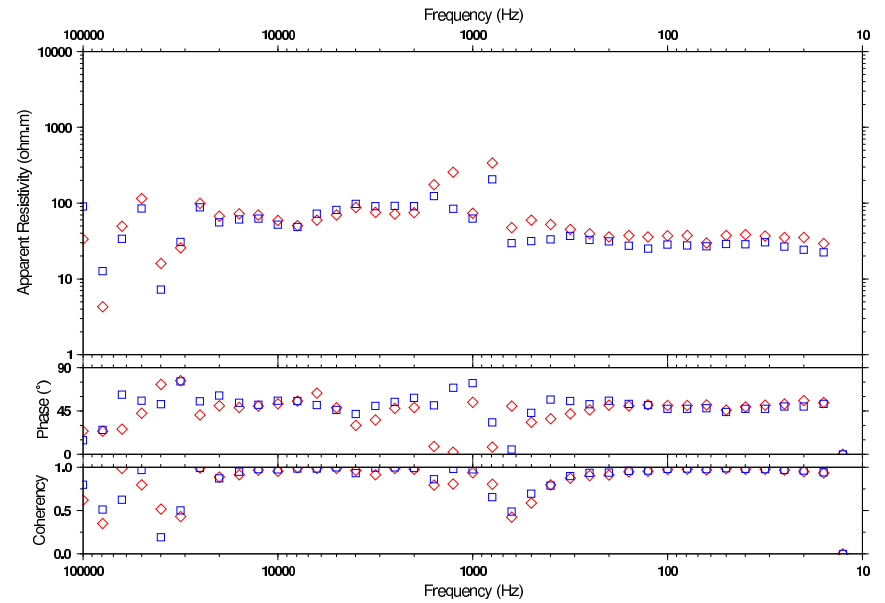
SVNA 06800m 035 - Scalar Res., Coherency, Phase (diamond=ExHy; square=EyHx)



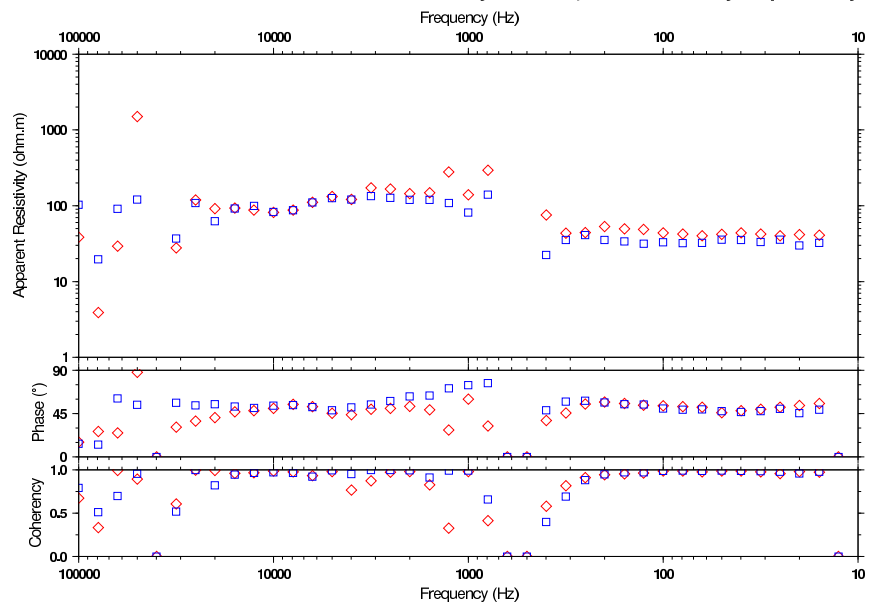
SVNA 06600m 068 - Scalar Res., Coherency, Phase (diamond=ExHy; square=EyHx)



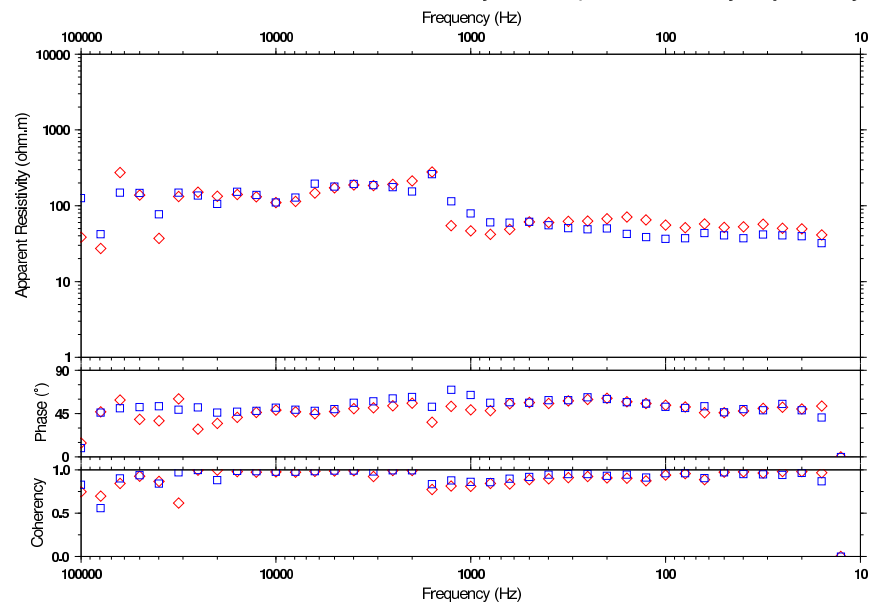
SVNA 07000m 069 - Scalar Res., Coherency, Phase (diamond=ExHy; square=EyHx)



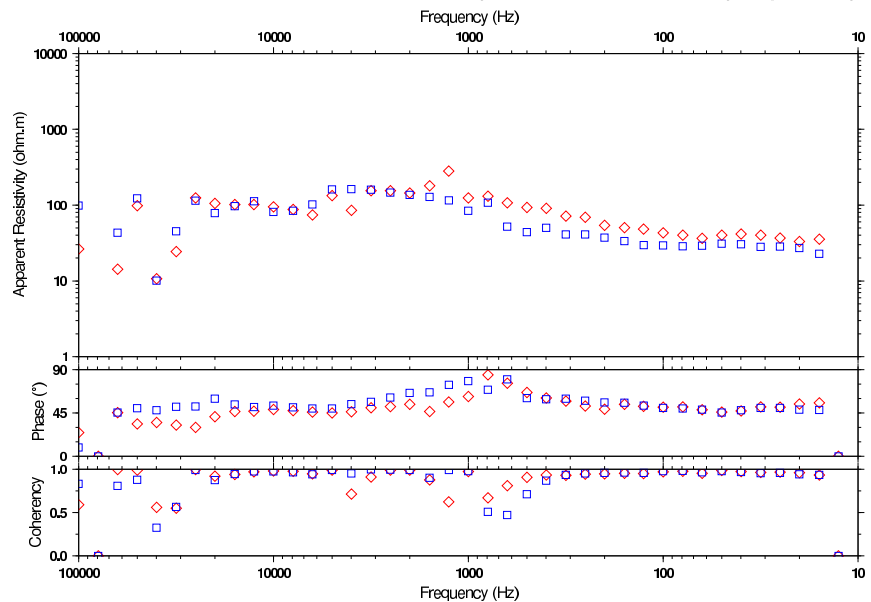
SVNA 07200m 095 - Scalar Res., Coherency, Phase (diamond=ExHy; square=EyHx)



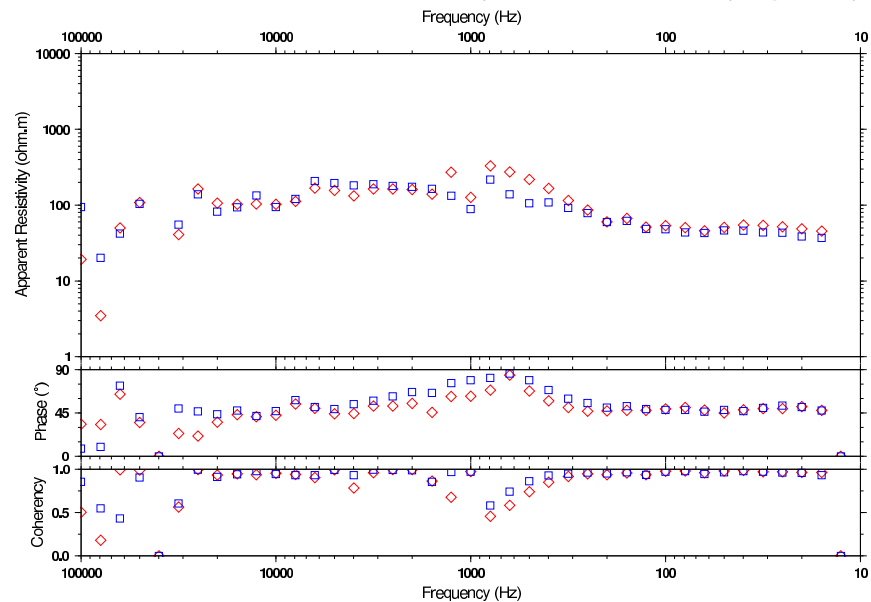
SVNA 07600m 039 - Scalar Res., Coherency, Phase (diamond=ExHy; square=EyHx)



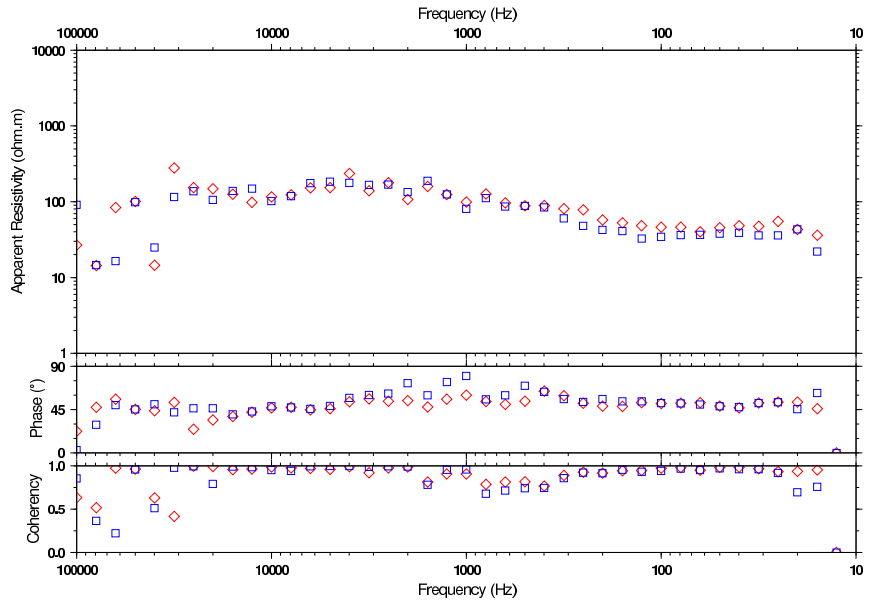
SVNA 07400m 070 - Scalar Res., Coherency, Phase (diamond=ExHy; square=EyHx)



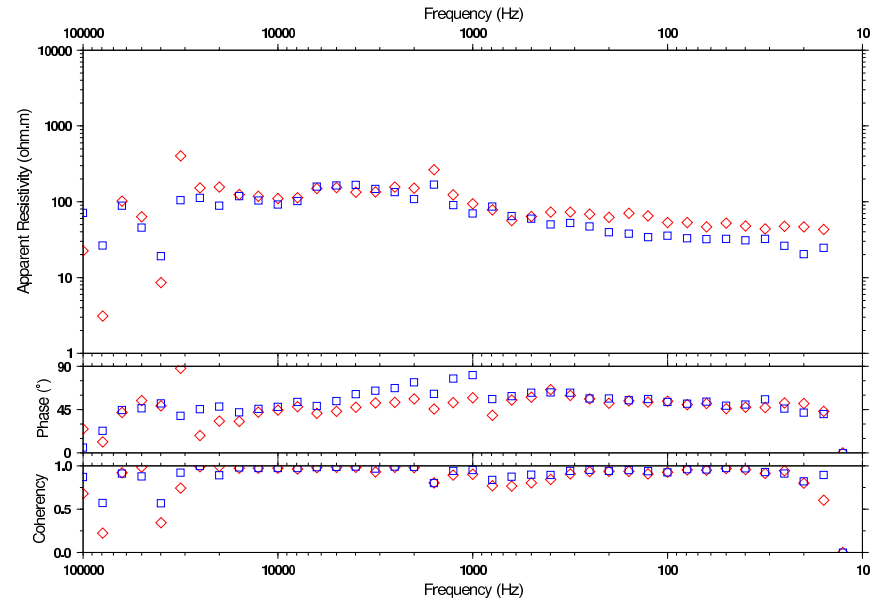
SVNA 07800m 071 - Scalar Res., Coherency, Phase (diamond=ExHy; square=EyHx)



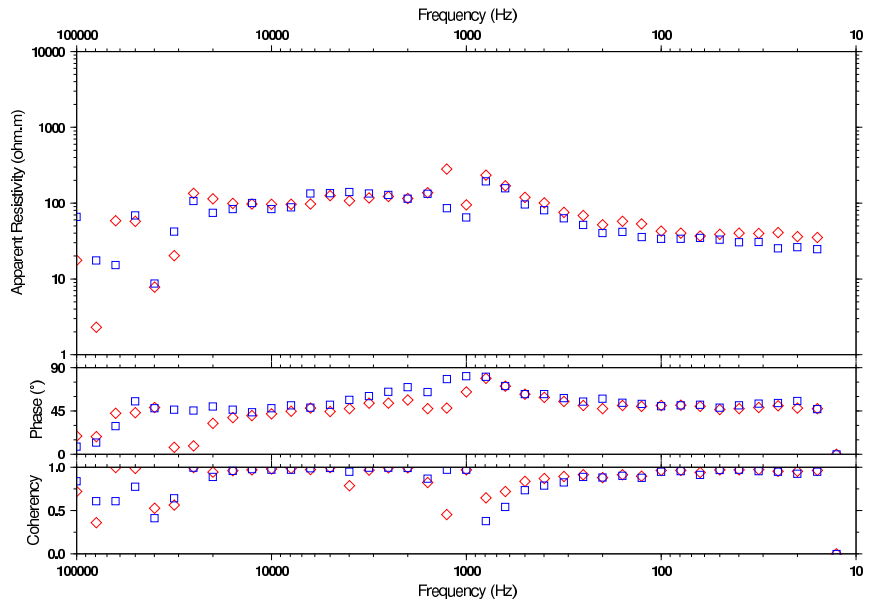
SVNA 08000m 040 - Scalar Res., Coherency, Phase (diamond=ExHy; square=EyHx)



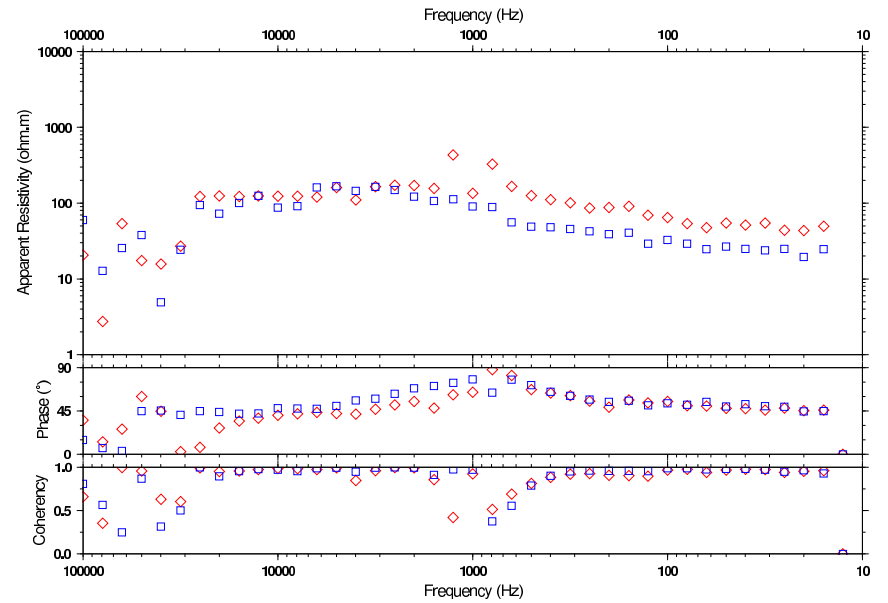
SVNA 08400m 041 - Scalar Res., Coherency, Phase (diamond=ExHy; square=EyHx)



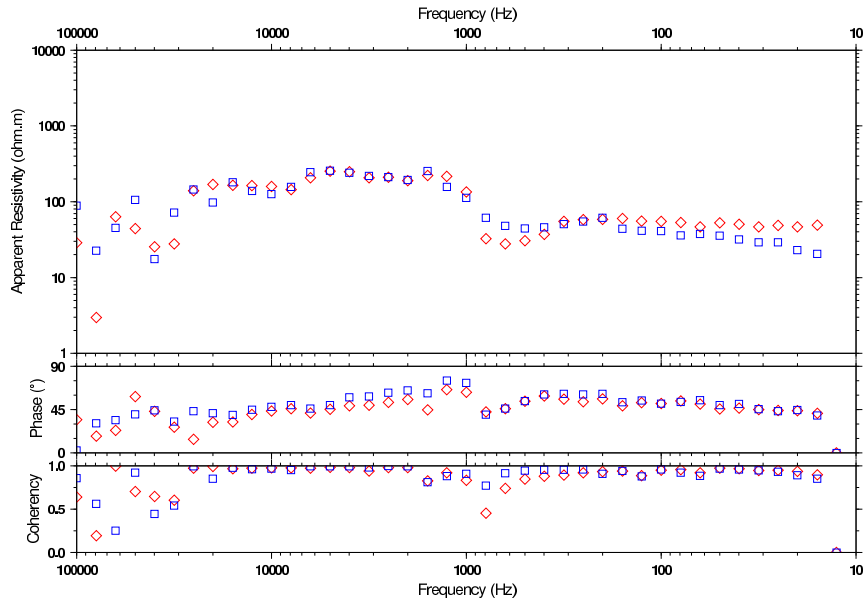
SVNA 08200m 072 - Scalar Res., Coherency, Phase (diamond=ExHy; square=EyHx)



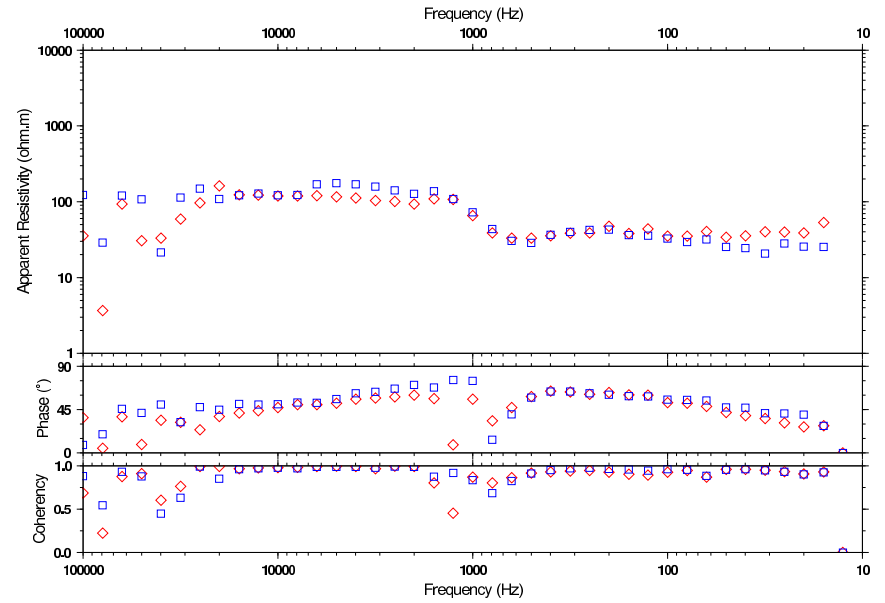
SVNA 08600m 074 - Scalar Res., Coherency, Phase (diamond=ExHy; square=EyHx)



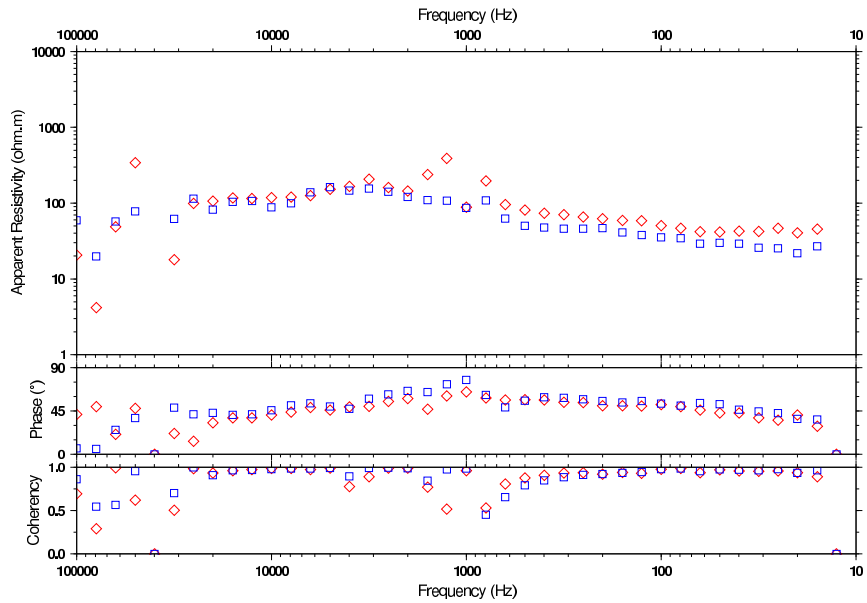
SVNA 08800m 043 - Scalar Res., Coherency, Phase (diamond=ExHy; square=EyHx)



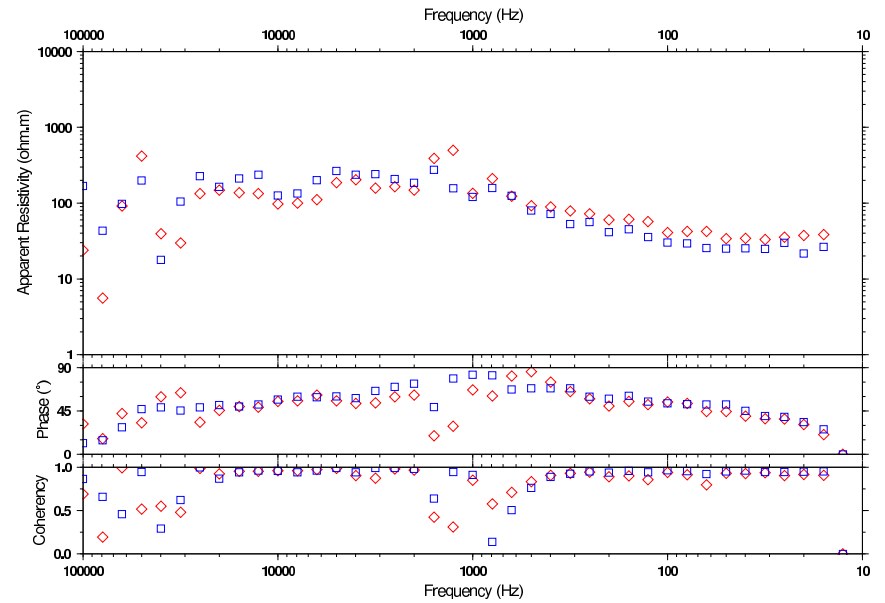
SVNA 09200m 045 - Scalar Res., Coherency, Phase (diamond=ExHy; square=EyHx)



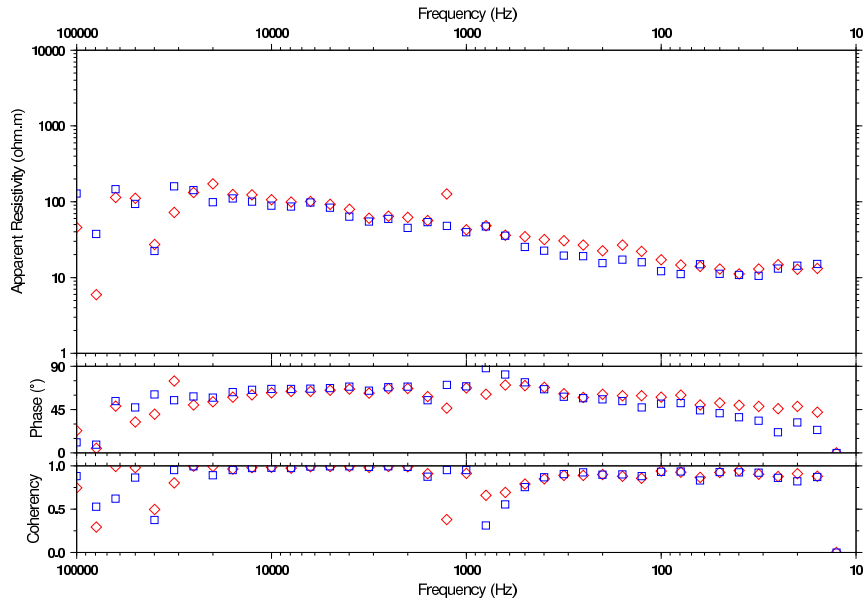
SVNA 09000m 075 - Scalar Res., Coherency, Phase (diamond=ExHy; square=EyHx)



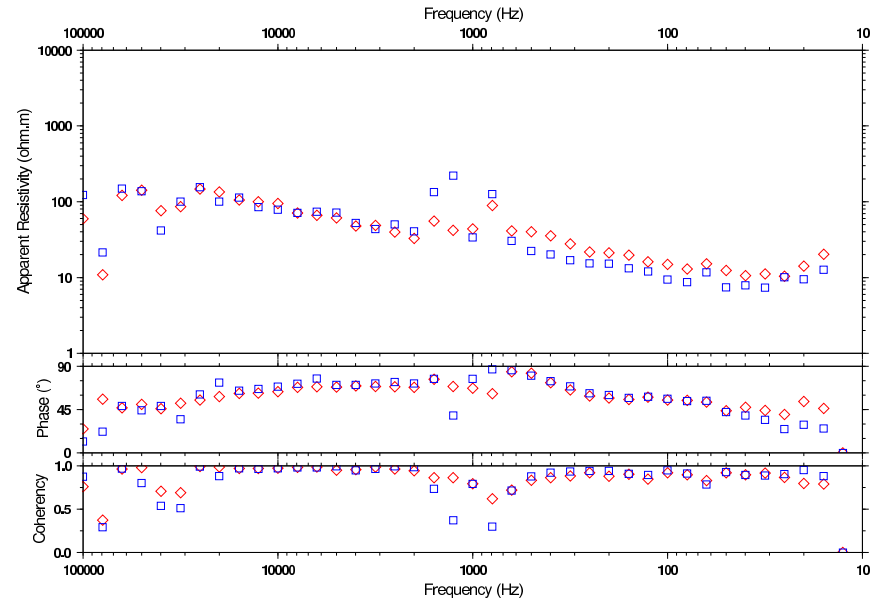
SVNA 09400m 077 - Scalar Res., Coherency, Phase (diamond=ExHy; square=EyHx)



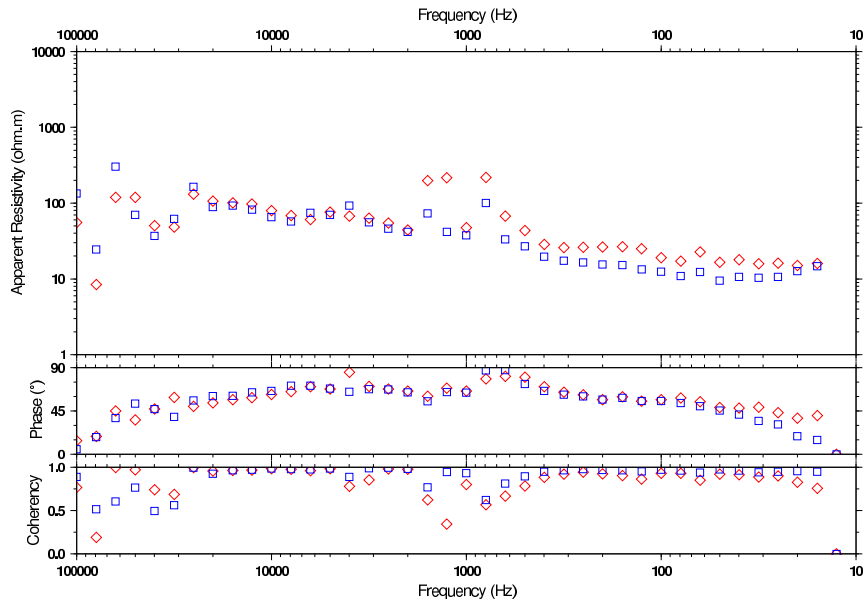
SVNA 09600m 046 - Scalar Res., Coherency, Phase (diamond=ExHy; square=EyHx)



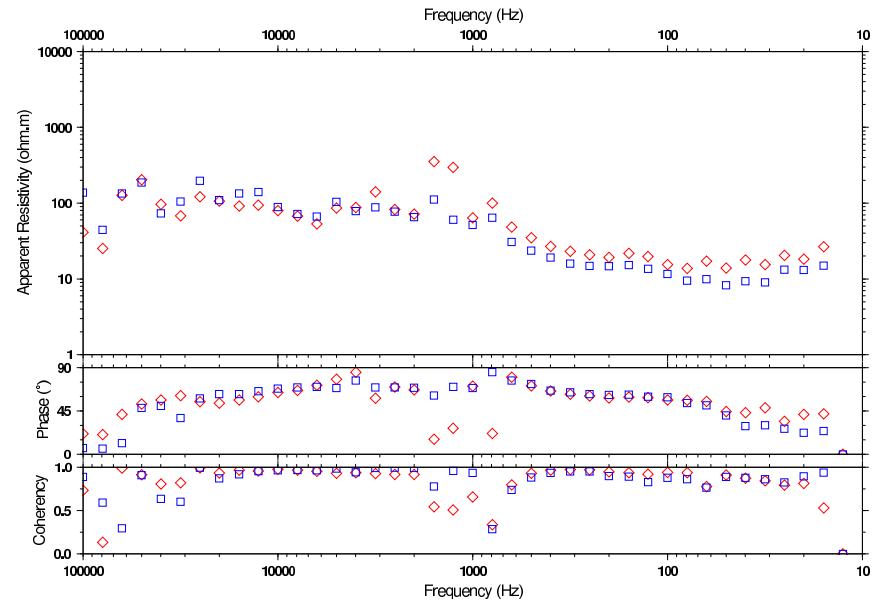
SVNA 10000m 047 - Scalar Res., Coherency, Phase (diamond=ExHy; square=EyHx)



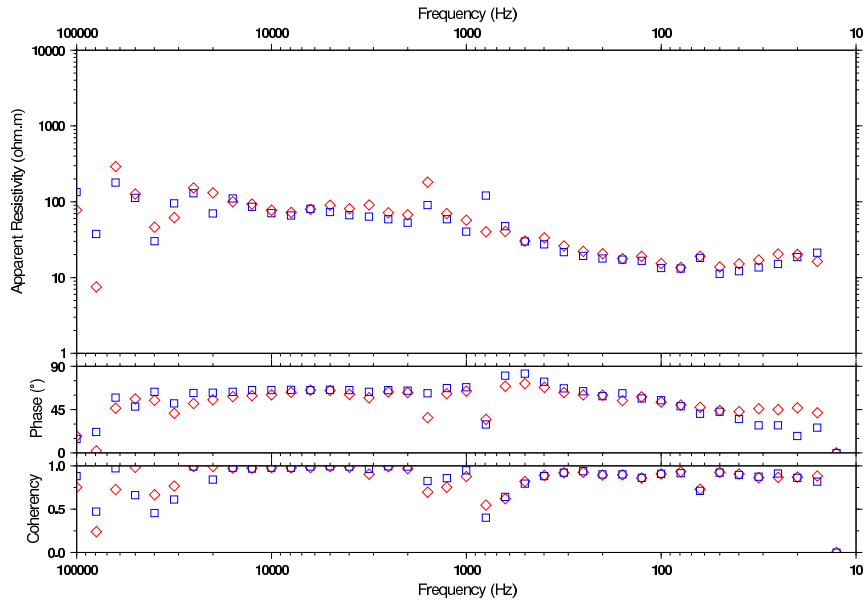
SVNA 09800m 078 - Scalar Res., Coherency, Phase (diamond=ExHy; square=EyHx)



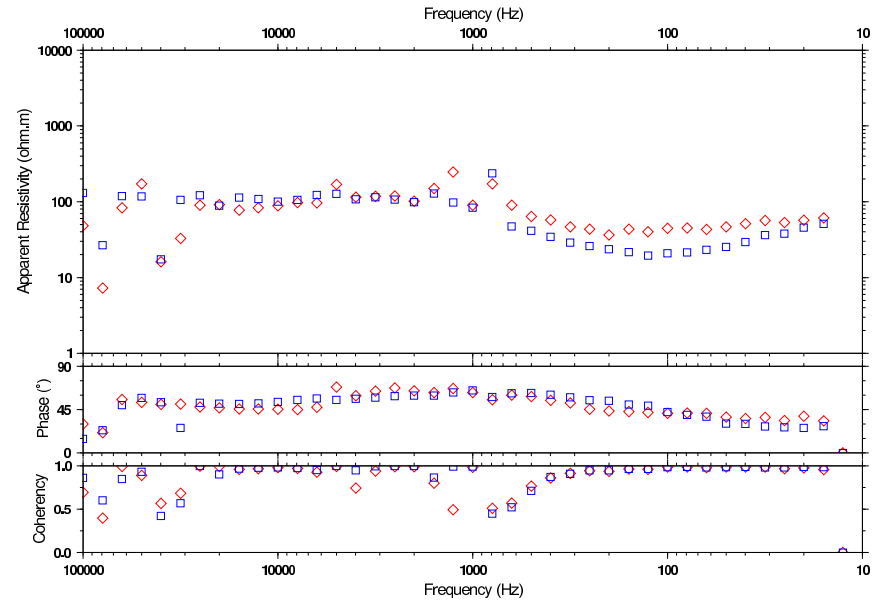
SVNA 10200m 080 - Scalar Res., Coherency, Phase (diamond=ExHy; square=EyHx)



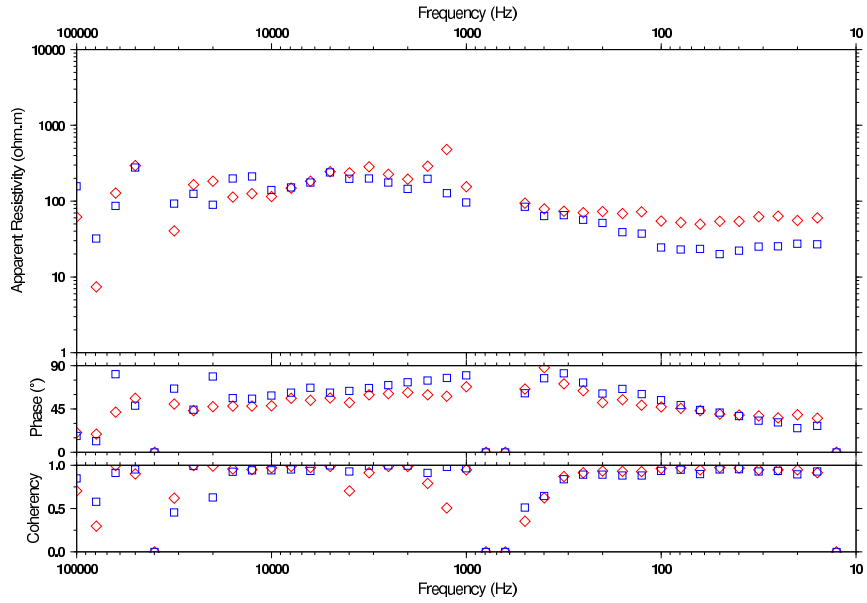
SVNA 10400m 049 - Scalar Res., Coherency, Phase (diamond=ExHy; square=EyHx)



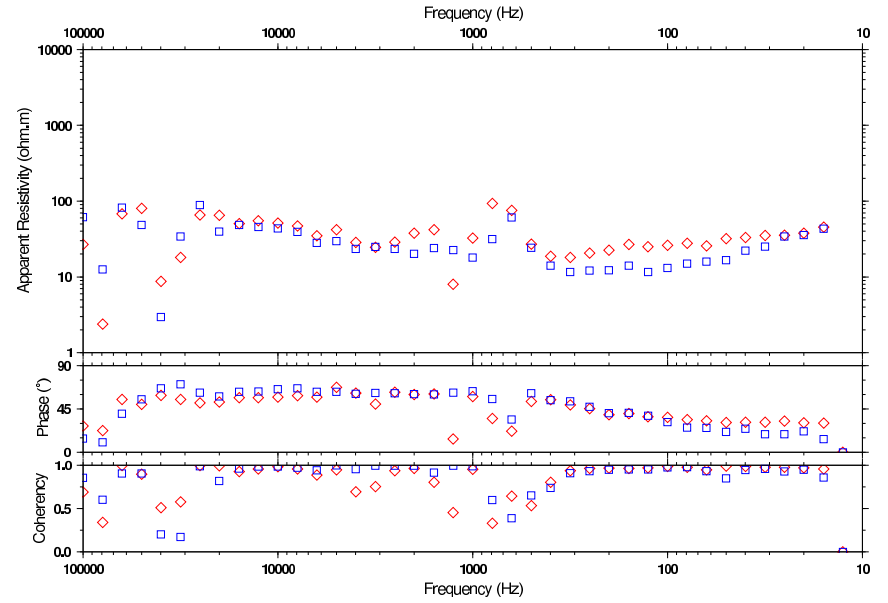
SVNA 10800m 051 - Scalar Res., Coherency, Phase (diamond=ExHy; square=EyHx)



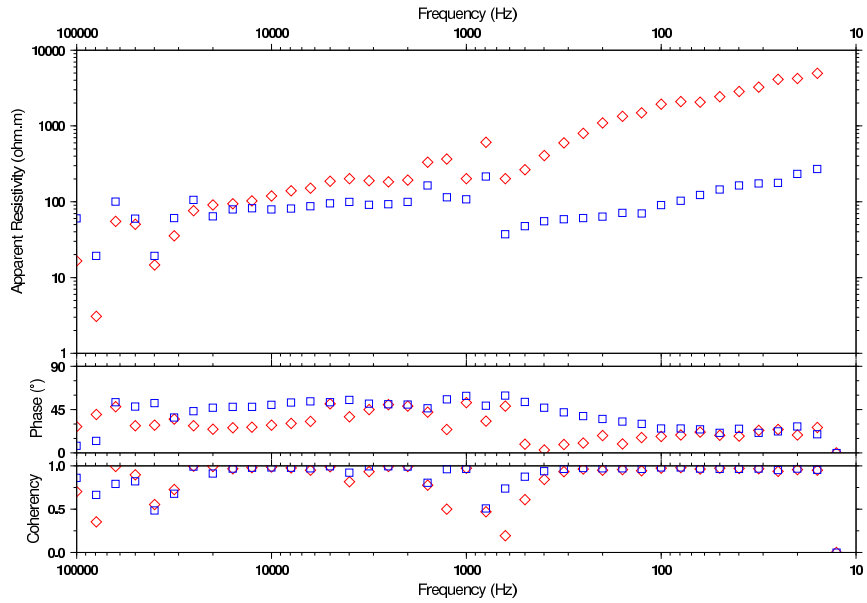
SVNA 10600m 082 - Scalar Res., Coherency, Phase (diamond=ExHy; square=EyHx)



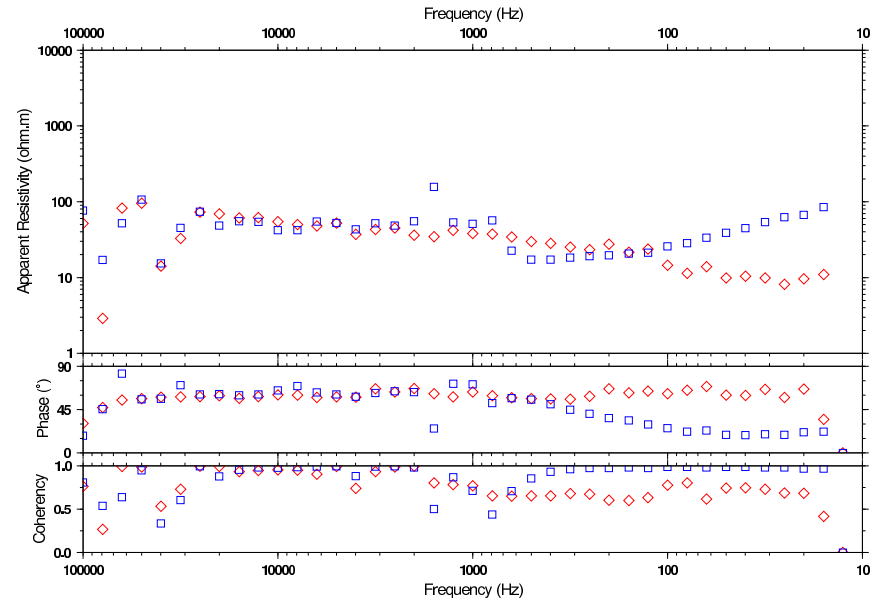
SVNA 11000m 083 - Scalar Res., Coherency, Phase (diamond=ExHy; square=EyHx)



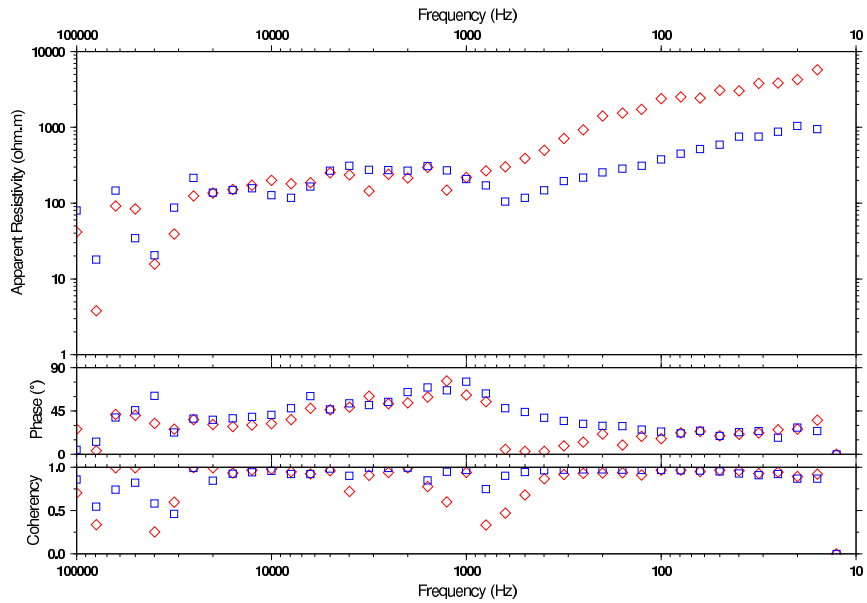
SVNA 11200m 052 - Scalar Res., Coherency, Phase (diamond=ExHy; square=EyHx)



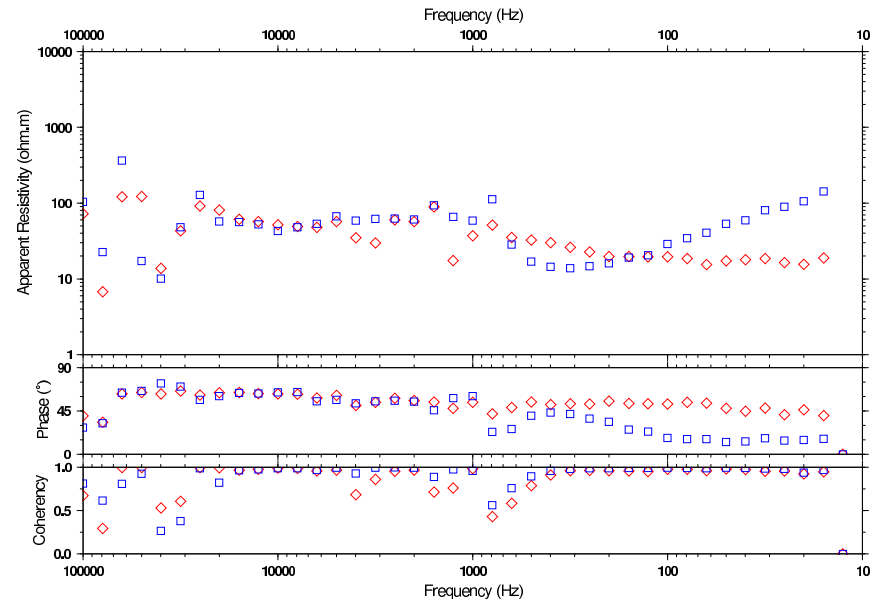
SVNA 11600m 098 - Scalar Res., Coherency, Phase (diamond=ExHy; square=EyHx)



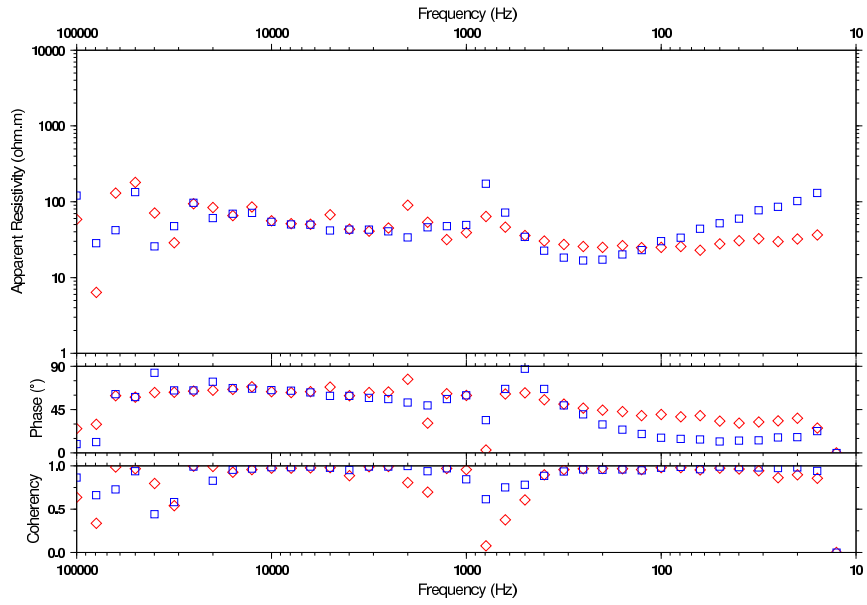
SVNA 11400m 084 - Scalar Res., Coherency, Phase (diamond=ExHy; square=EyHx)



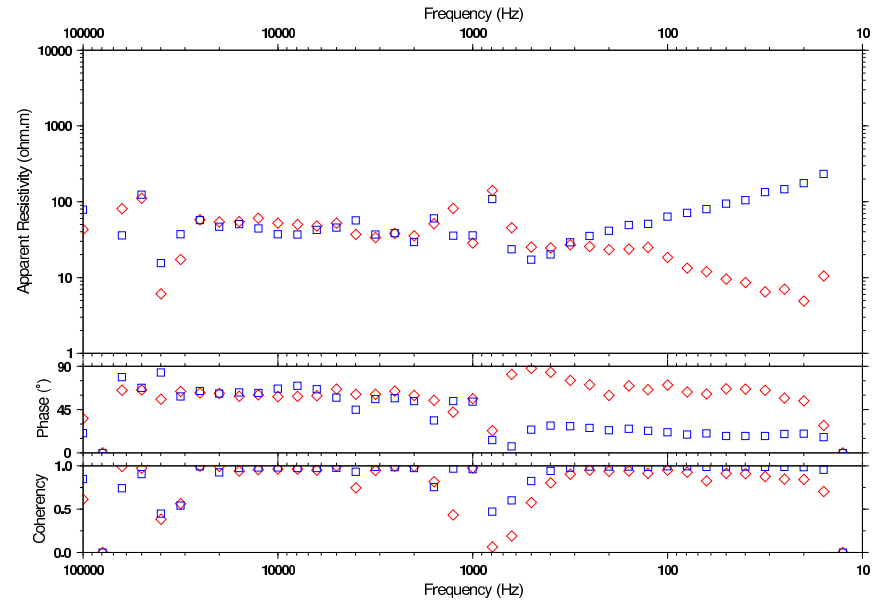
SVNA 11800m 087 - Scalar Res., Coherency, Phase (diamond=ExHy; square=EyHx)



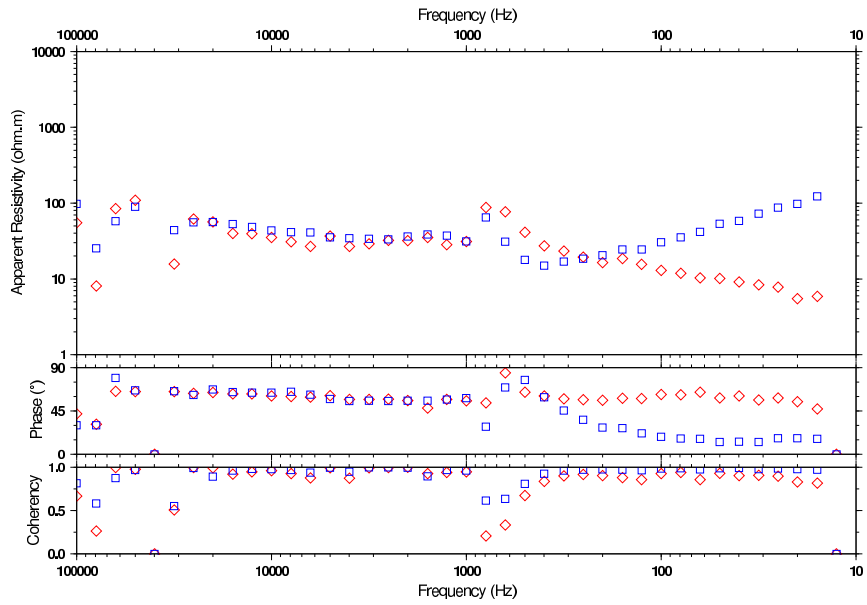
SVNA 12000m 094 - Scalar Res., Coherency, Phase (diamond=ExHy; square=EyHx)



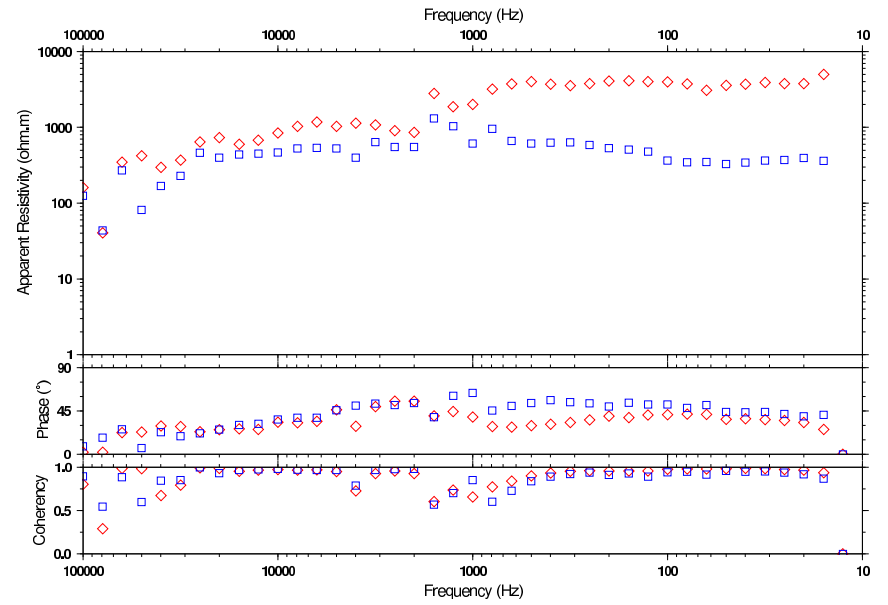
SVNA 12400m 093 - Scalar Res., Coherency, Phase (diamond=ExHy; square=EyHx)



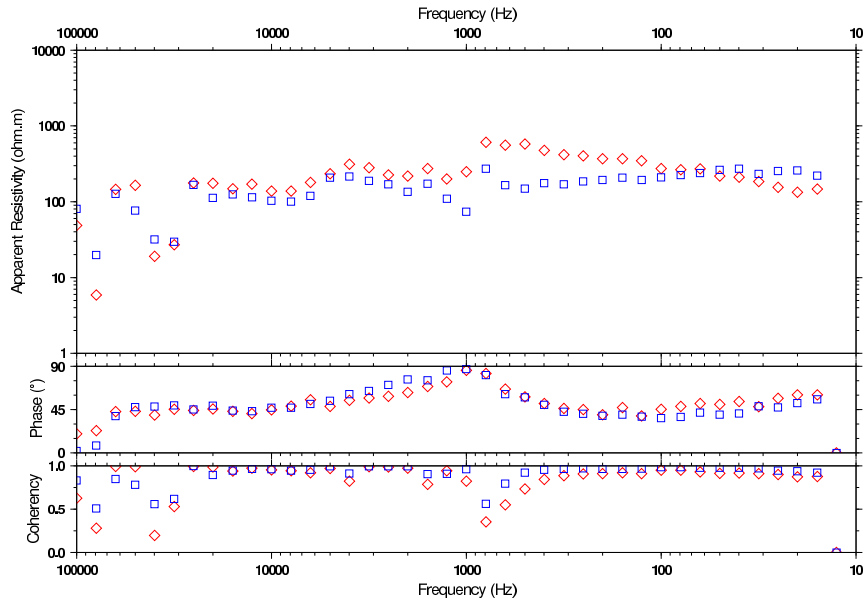
SVNA 12200m 088 - Scalar Res., Coherency, Phase (diamond=ExHy; square=EyHx)



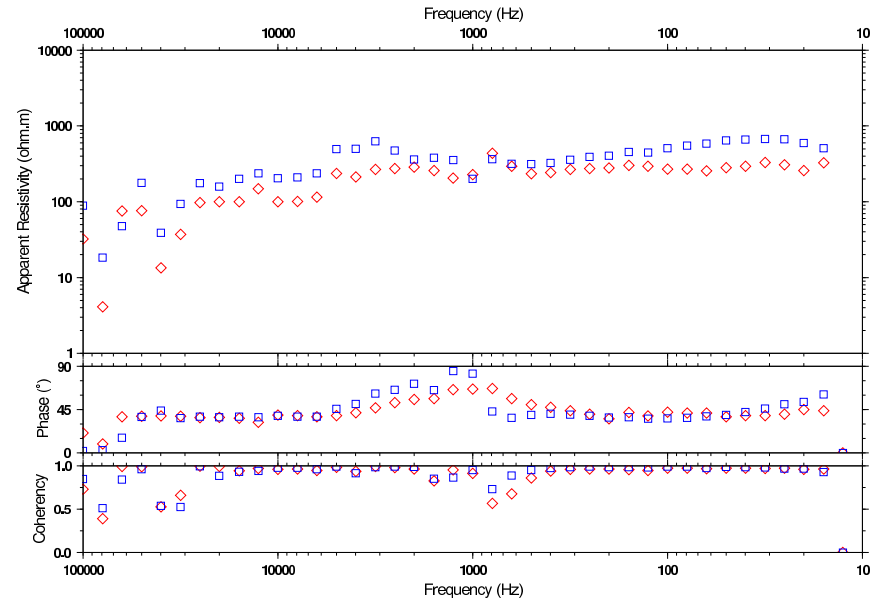
SVNA 12600m 102 - Scalar Res., Coherency, Phase (diamond=ExHy; square=EyHx)



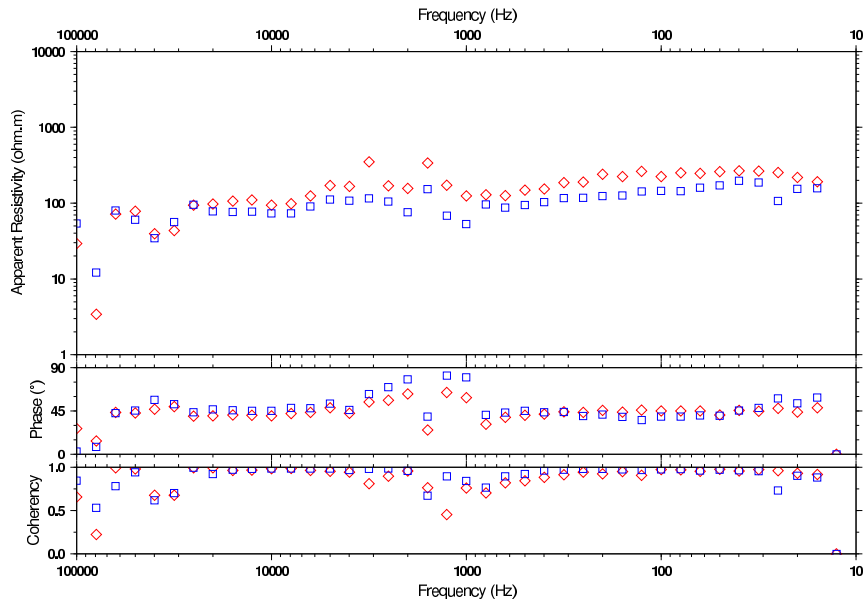
SVNB -0200m 107 - Scalar Res., Coherency, Phase (diamond=ExHy; square=EyHx)



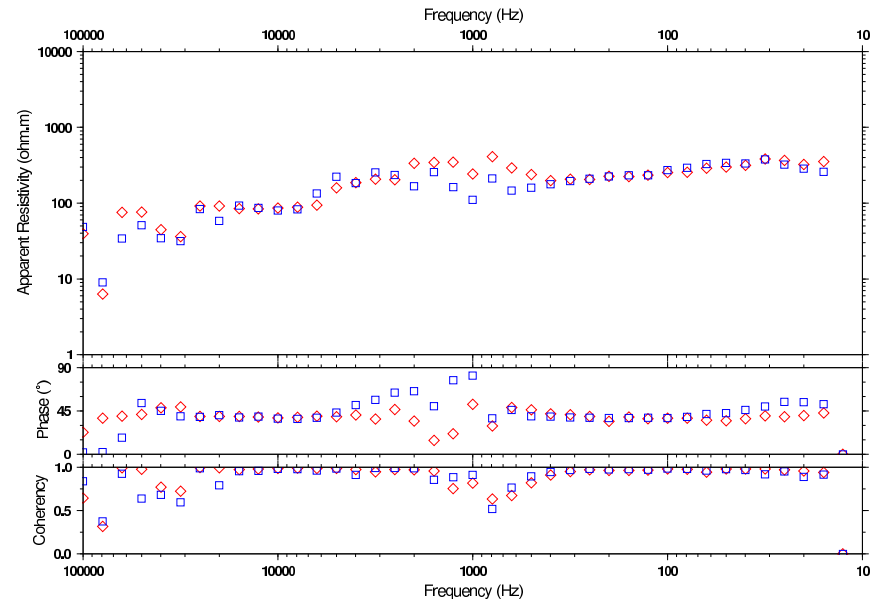
SVNB 00200m 108 - Scalar Res., Coherency, Phase (diamond=ExHy; square=EyHx)



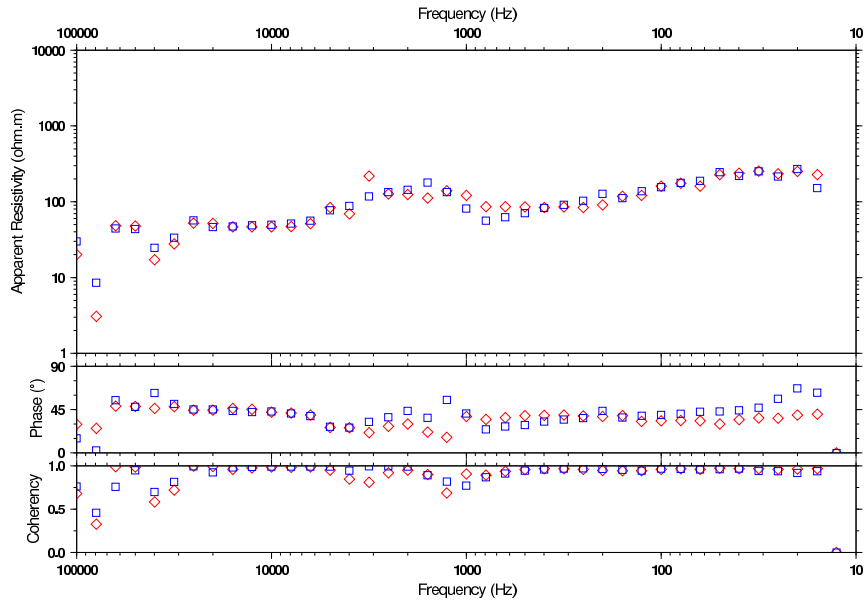
SVNB 00000m 103 - Scalar Res., Coherency, Phase (diamond=ExHy; square=EyHx)



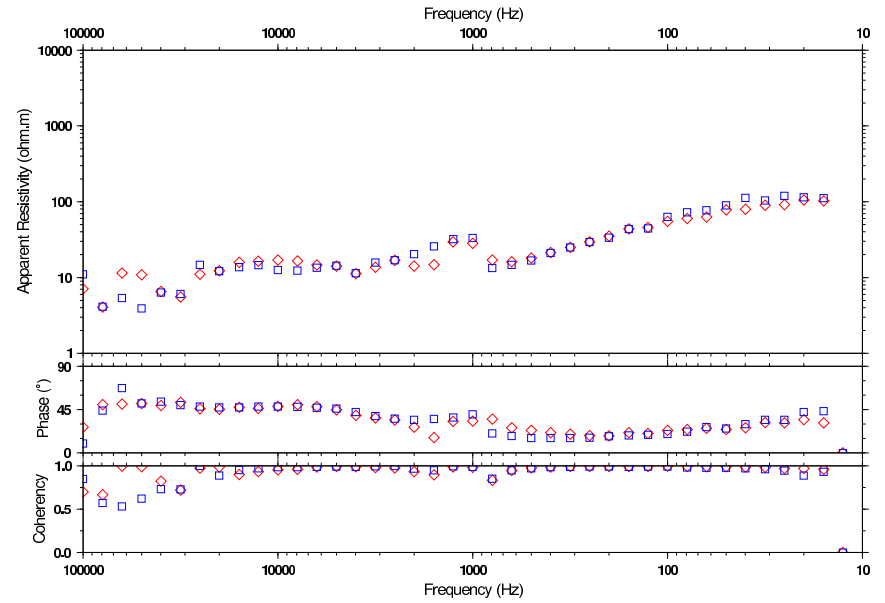
SVNB 00400m 104 - Scalar Res., Coherency, Phase (diamond=ExHy; square=EyHx)



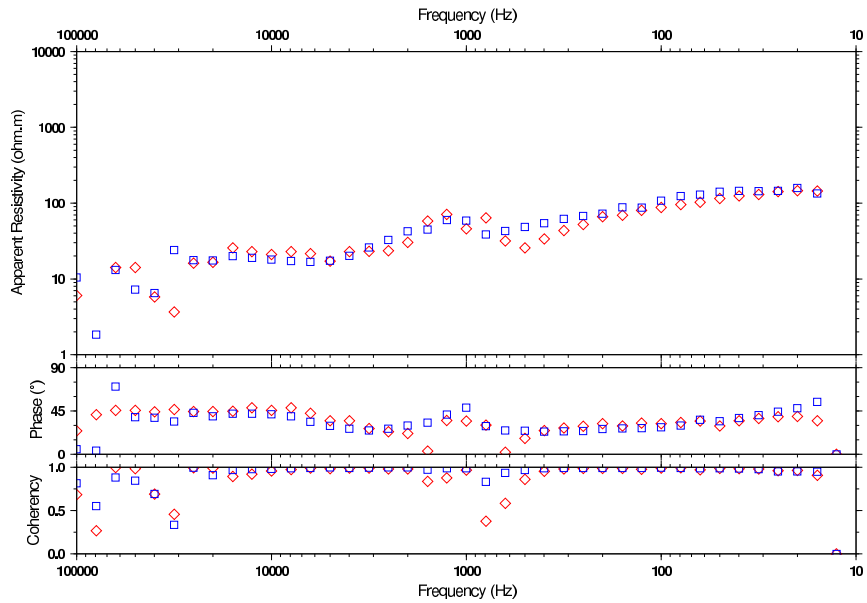
SVNB 00600m 109 - Scalar Res., Coherency, Phase (diamond=ExHy; square=EyHx)



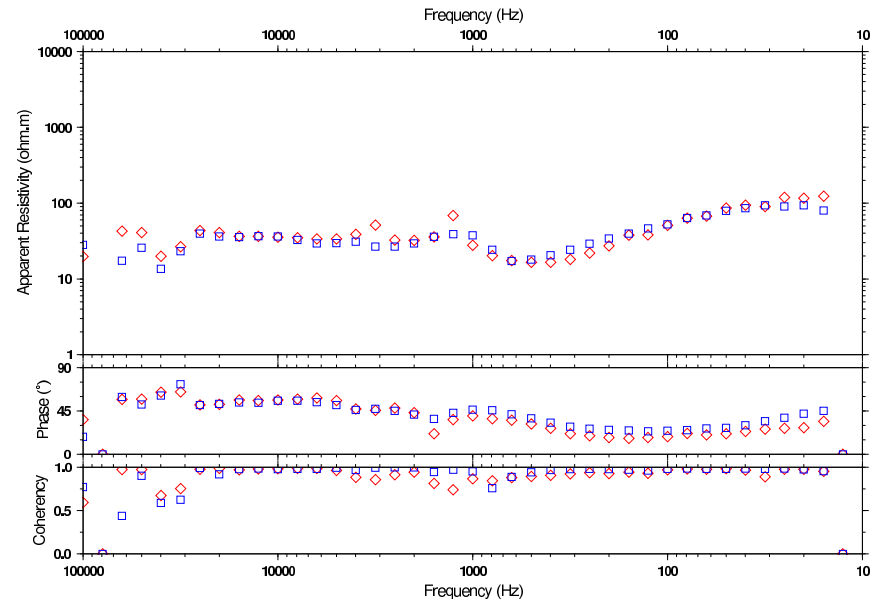
SVNB 01200m 106 - Scalar Res., Coherency, Phase (diamond=ExHy; square=EyHx)



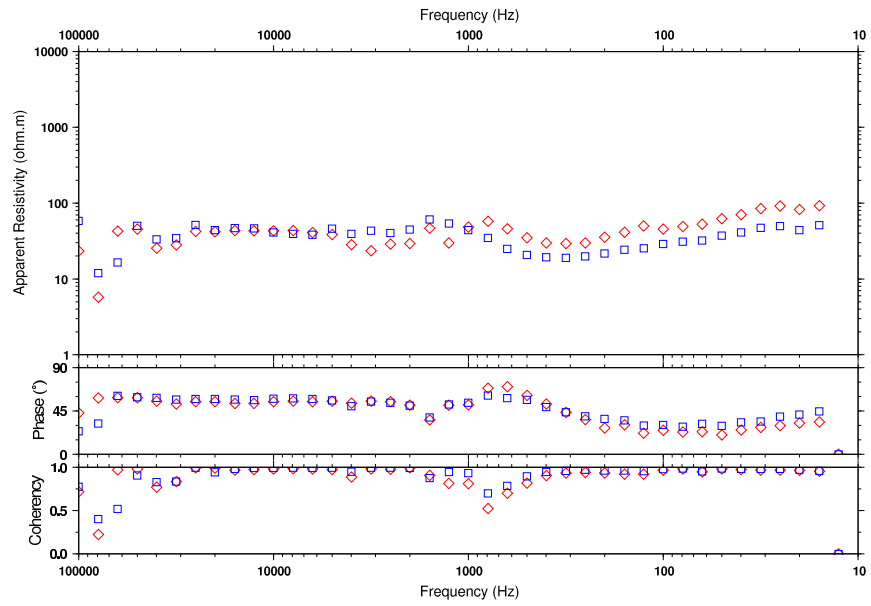
SVNB 00800m 105 - Scalar Res., Coherency, Phase (diamond=ExHy; square=EyHx)



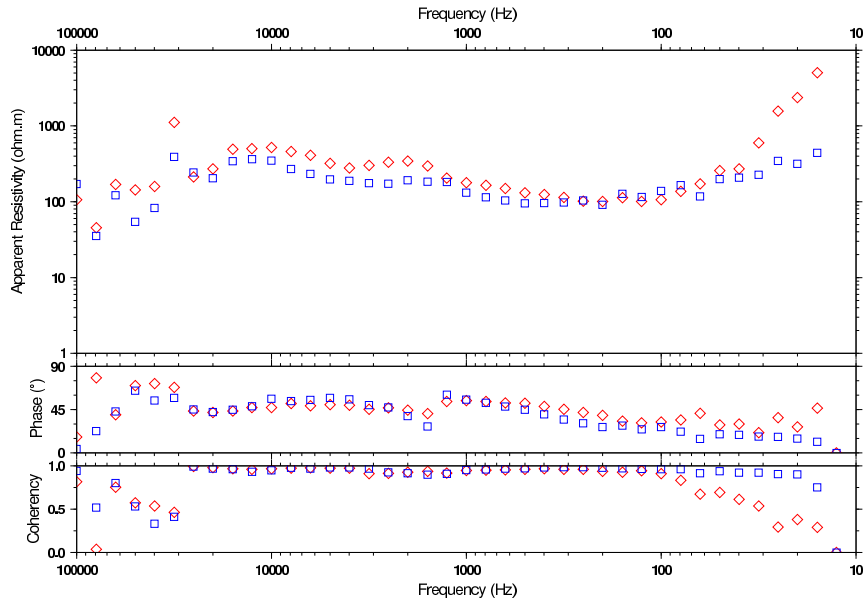
SVNB 01600m 111 - Scalar Res., Coherency, Phase (diamond=ExHy; square=EyHx)



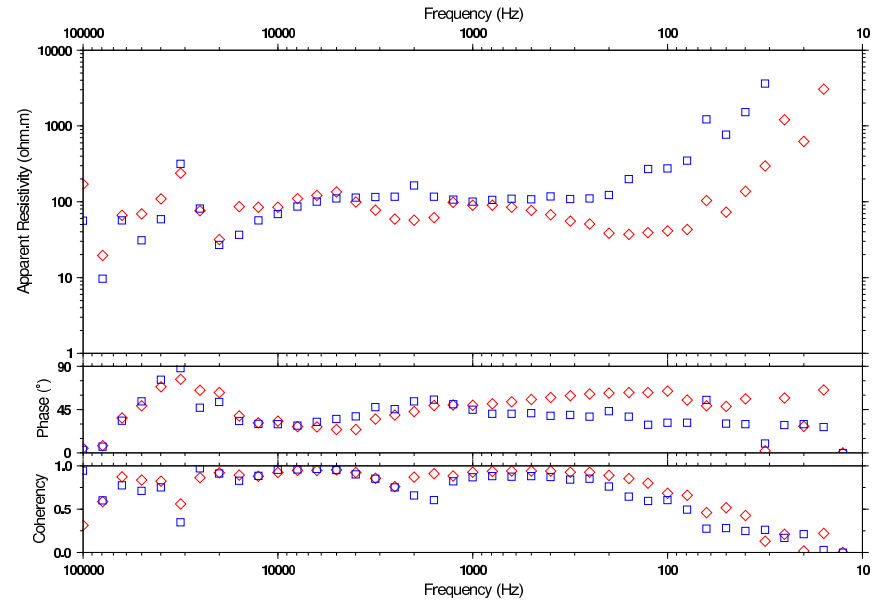
SVNB 02000m 112 - Scalar Res., Coherency, Phase (diamond=ExHy; square=EyHx)



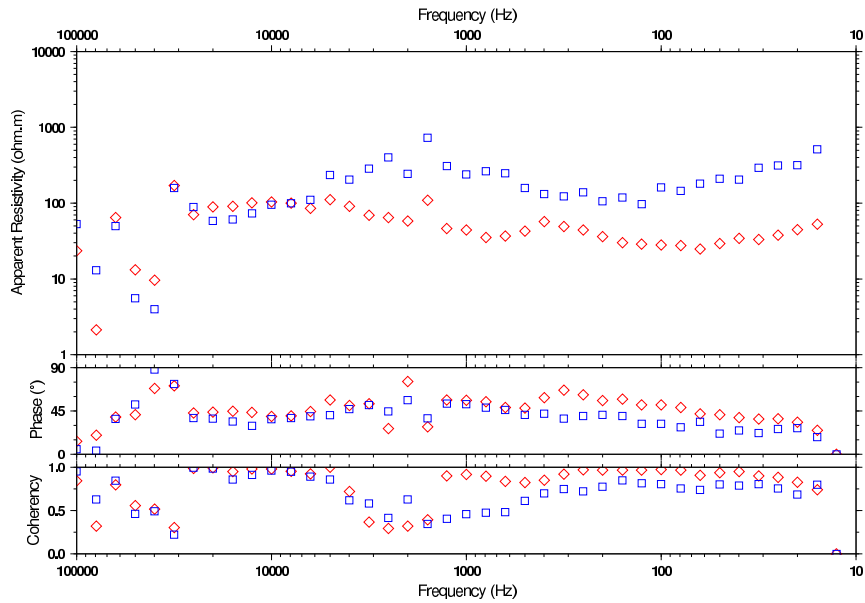
SVNC -0600m 016 - Scalar Res., Coherency, Phase (diamond=ExHy; square=EyHx)



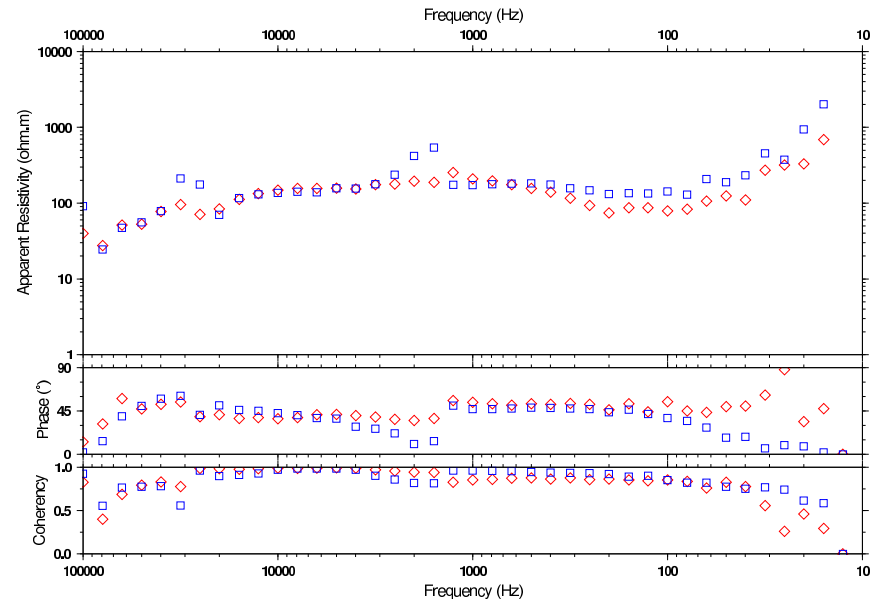
SVNC -0200m 019 - Scalar Res., Coherency, Phase (diamond=ExHy; square=EyHx)



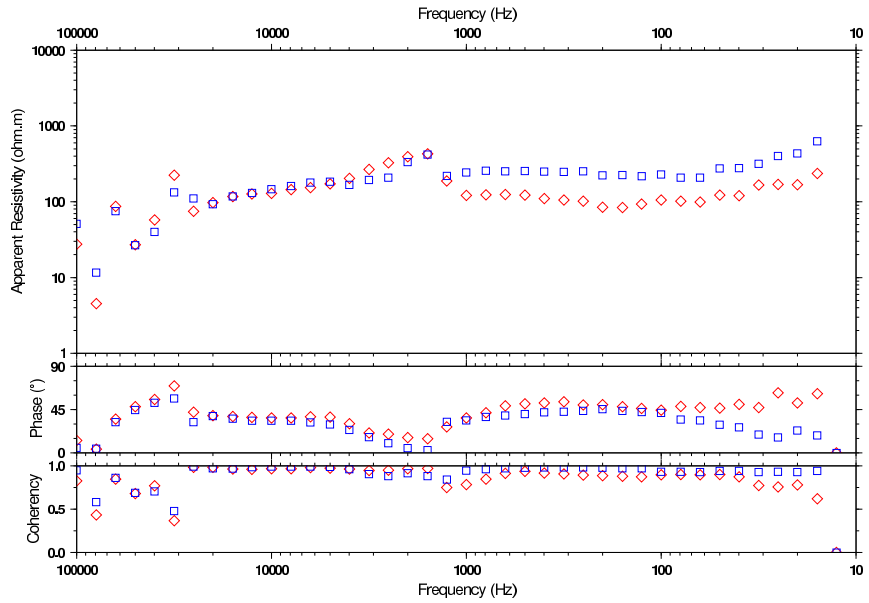
SVNC -0400m 027 - Scalar Res., Coherency, Phase (diamond=ExHy; square=EyHx)



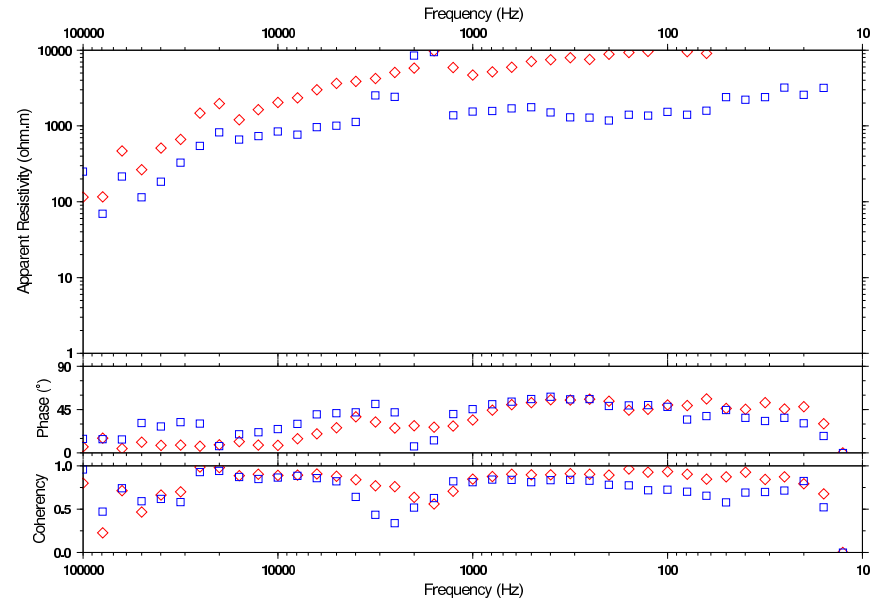
SVNC 0000m 021 - Scalar Res., Coherency, Phase (diamond=ExHy; square=EyHx)



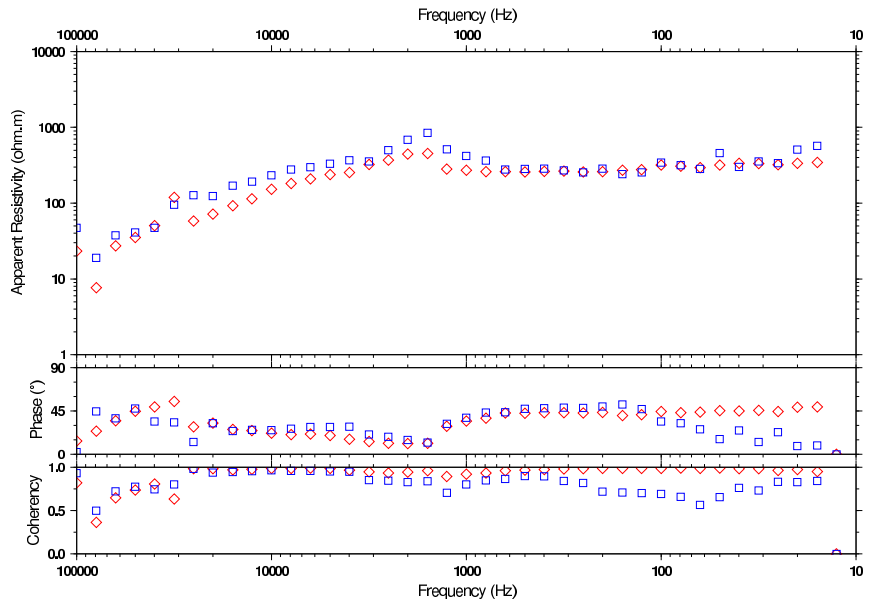
SVNC 00100m 033 - Scalar Res., Coherency, Phase (diamond=ExHy; square=EyHx)



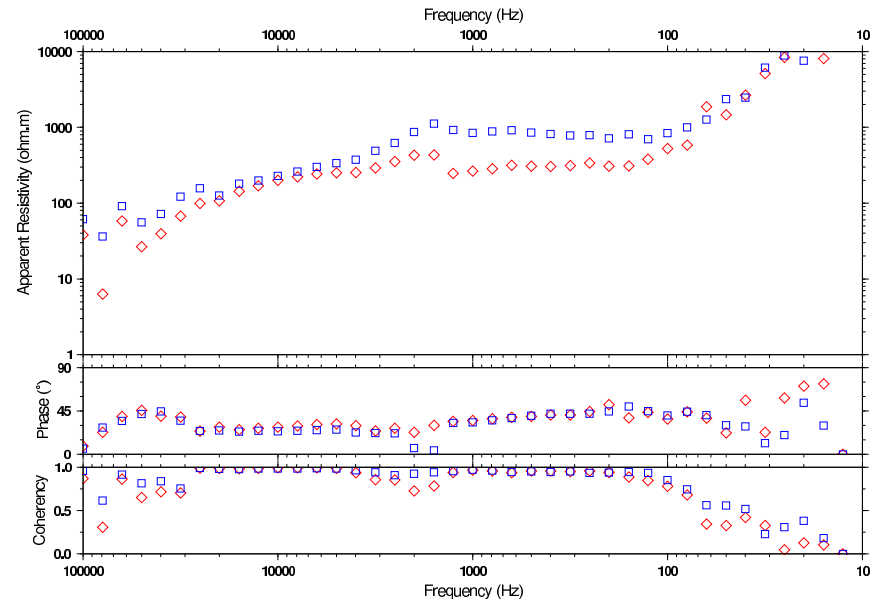
SVNC 00400m 023 - Scalar Res., Coherency, Phase (diamond=ExHy; square=EyHx)



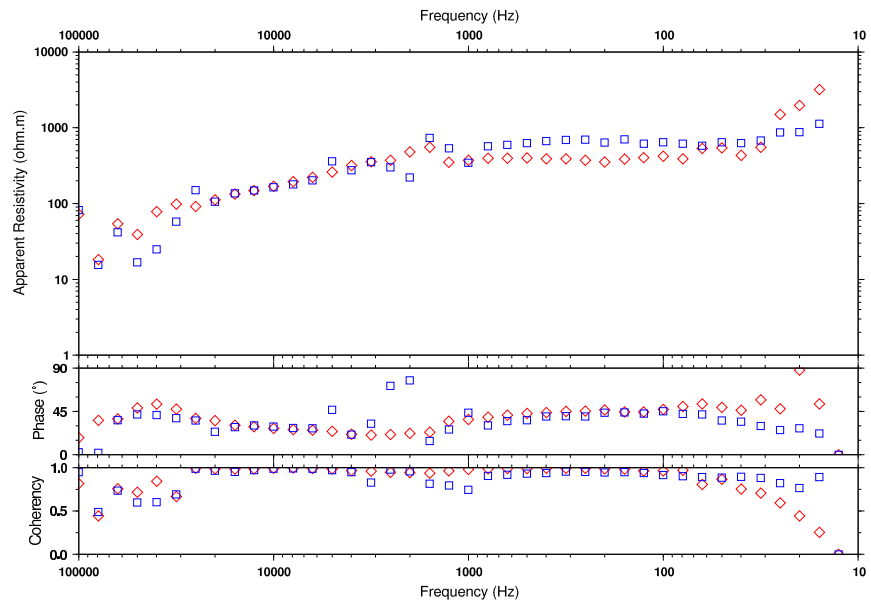
SVNC 00200m 032 - Scalar Res., Coherency, Phase (diamond=ExHy; square=EyHx)



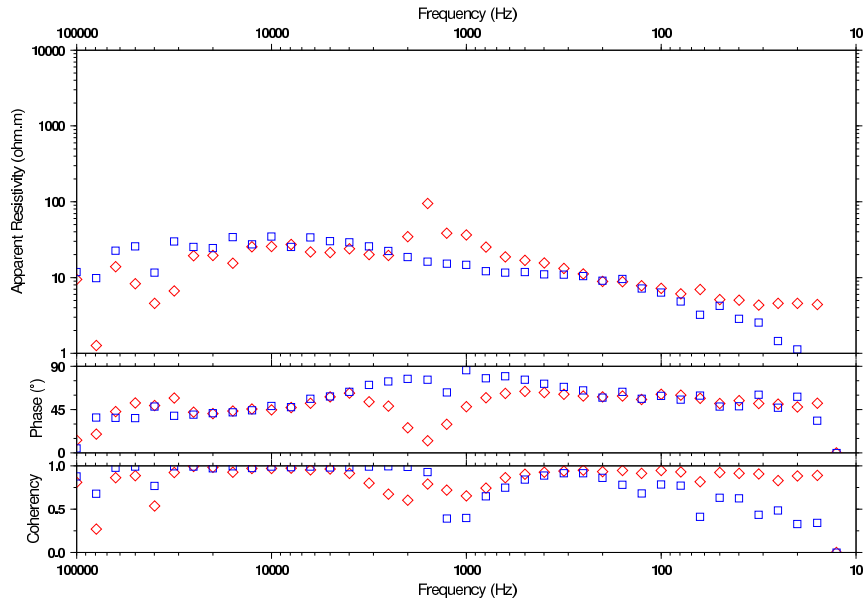
SVNC 00600m 025 - Scalar Res., Coherency, Phase (diamond=ExHy; square=EyHx)



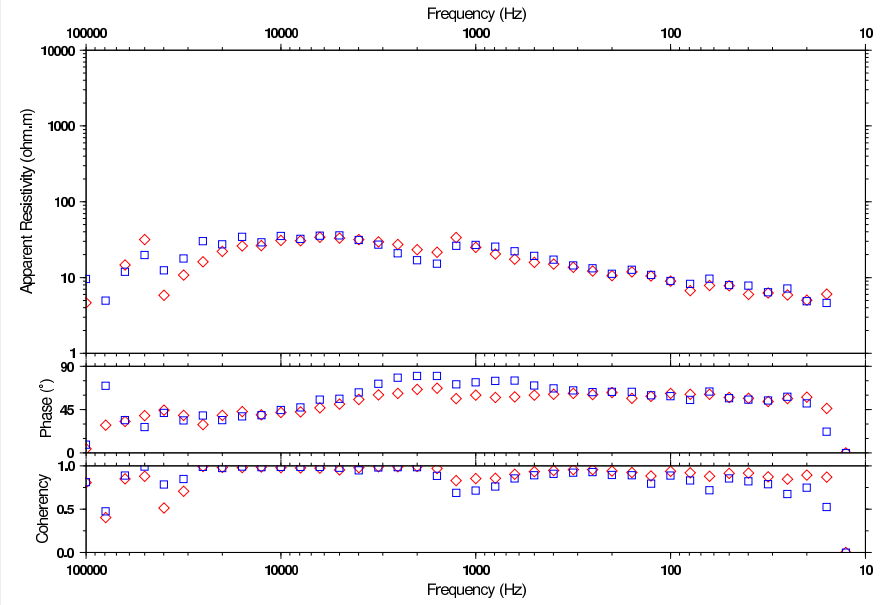
SVNC 00800m 030 - Scalar Res., Coherency, Phase (diamond=ExHy; square=EyHx)



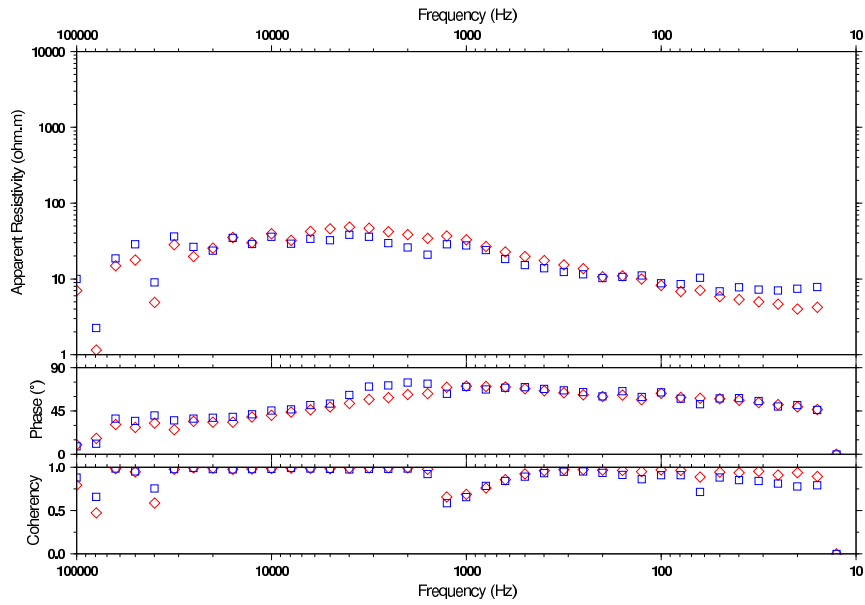
SVNE -1800m 016 - Scalar Res., Coherency, Phase (diamond=ExHy; square=EyHx)



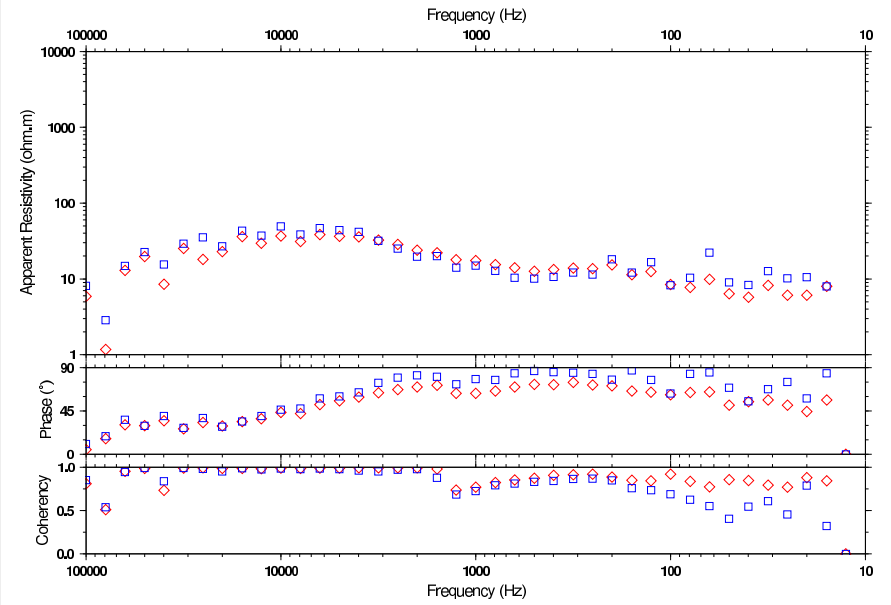
SVNE -1000m 013 - Scalar Res., Coherency, Phase (diamond=ExHy; square=EyHx)



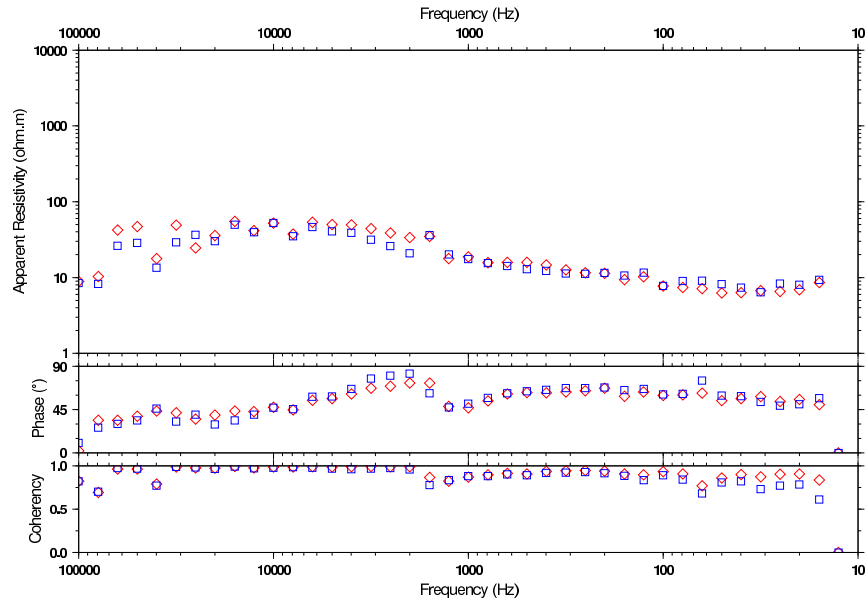
SVNE -1400m 014 - Scalar Res., Coherency, Phase (diamond=ExHy; square=EyHx)



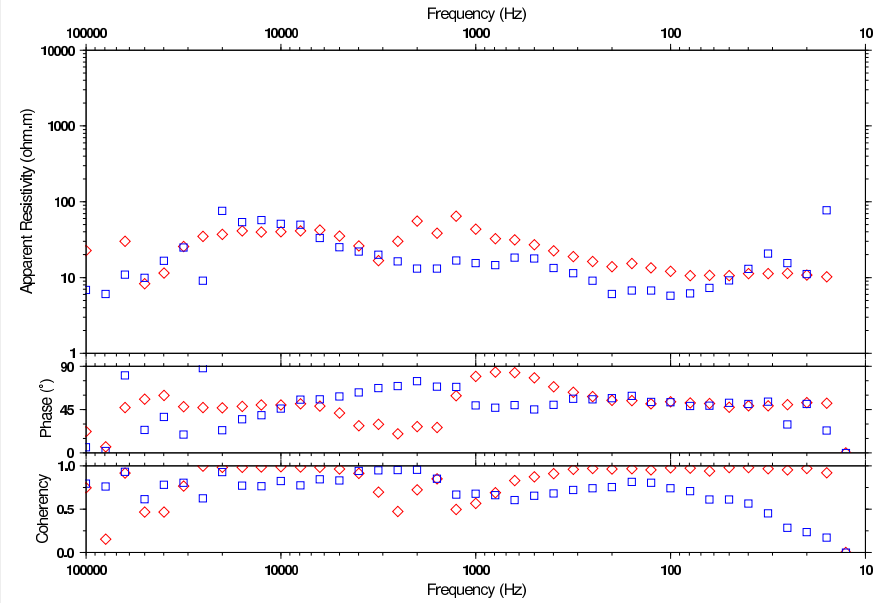
SVNE -0800m 012 - Scalar Res., Coherency, Phase (diamond=ExHy; square=EyHx)



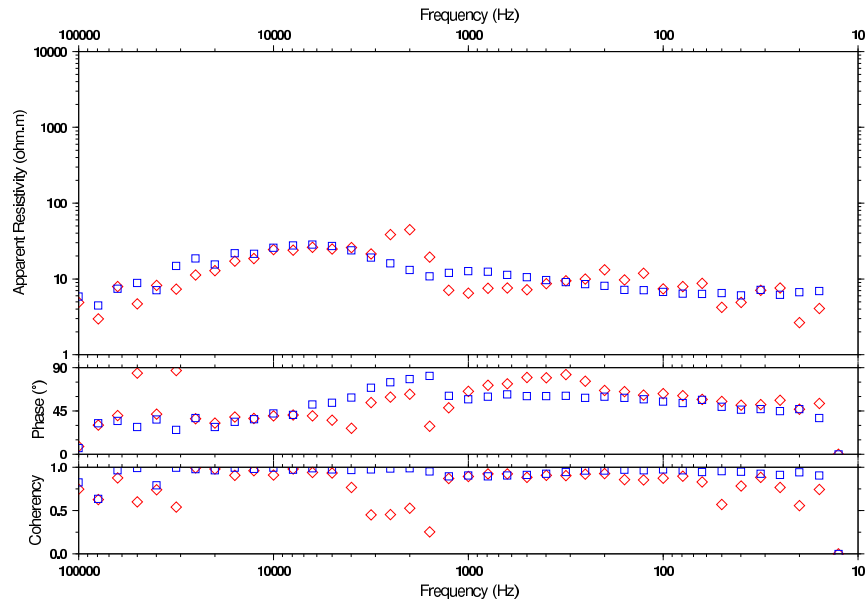
SVNE -0600m 010 - Scalar Res., Coherency, Phase (diamond=ExHy; square=EyHx)



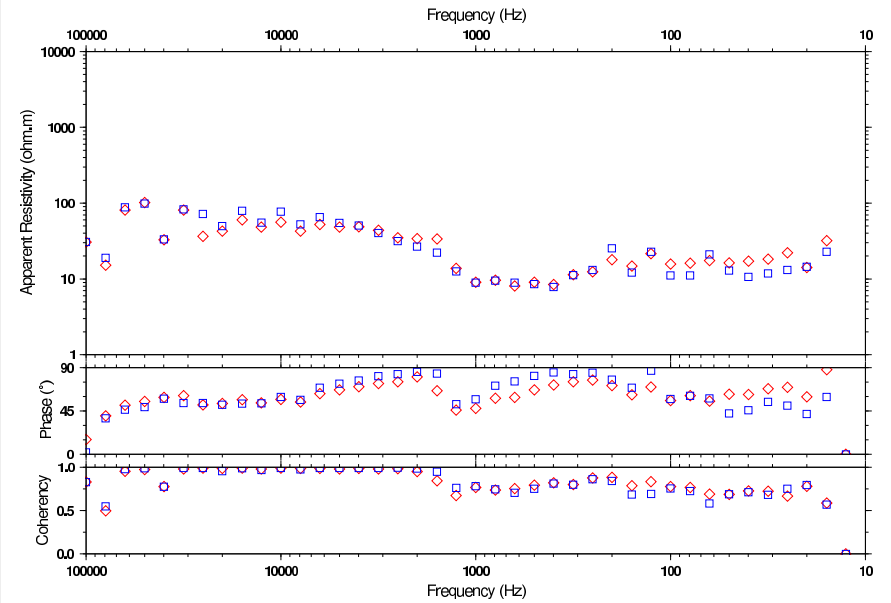
SVNE -0200m 041 - Scalar Res., Coherency, Phase (diamond=ExHy; square=EyHx)



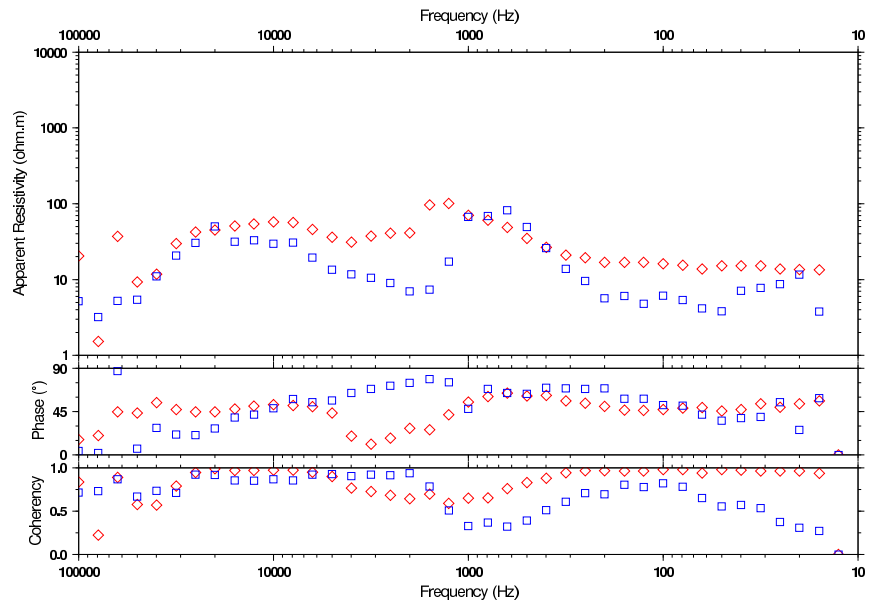
SVNE -0400m 007 - Scalar Res., Coherency, Phase (diamond=ExHy; square=EyHx)



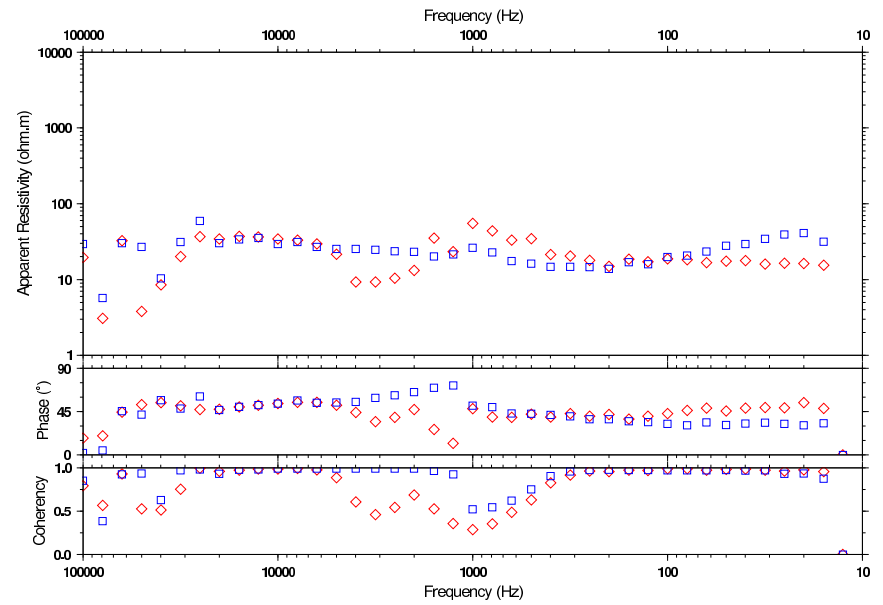
SVNE 0000m 004 - Scalar Res., Coherency, Phase (diamond=ExHy; square=EyHx)



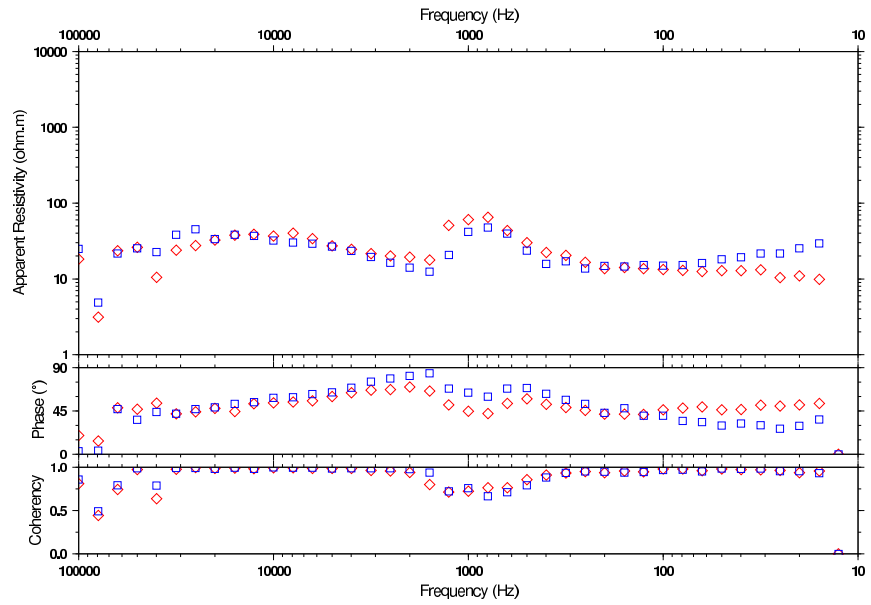
SVNE 00200m 039 - Scalar Res., Coherency, Phase (diamond=ExHy; square=EyHx)



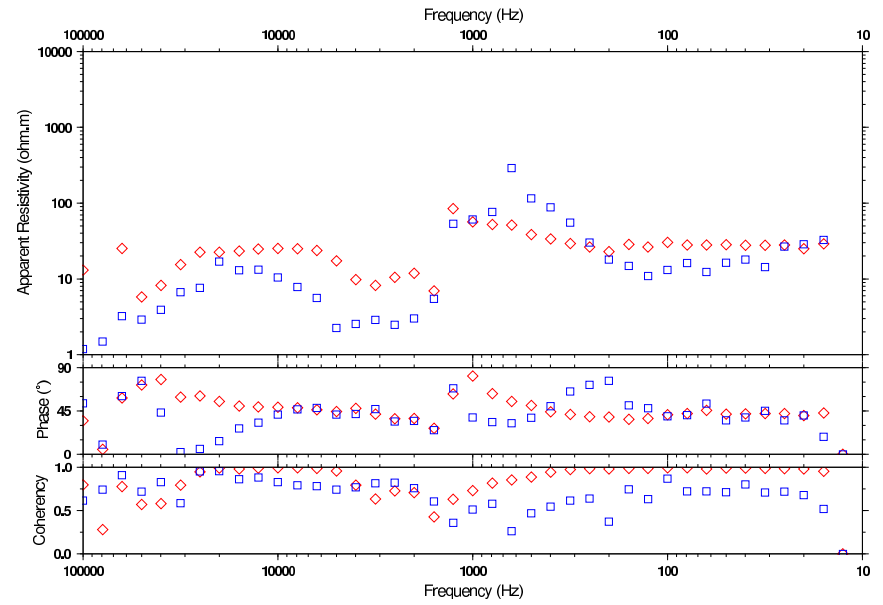
SVNE 00600m 023 - Scalar Res., Coherency, Phase (diamond=ExHy; square=EyHx)



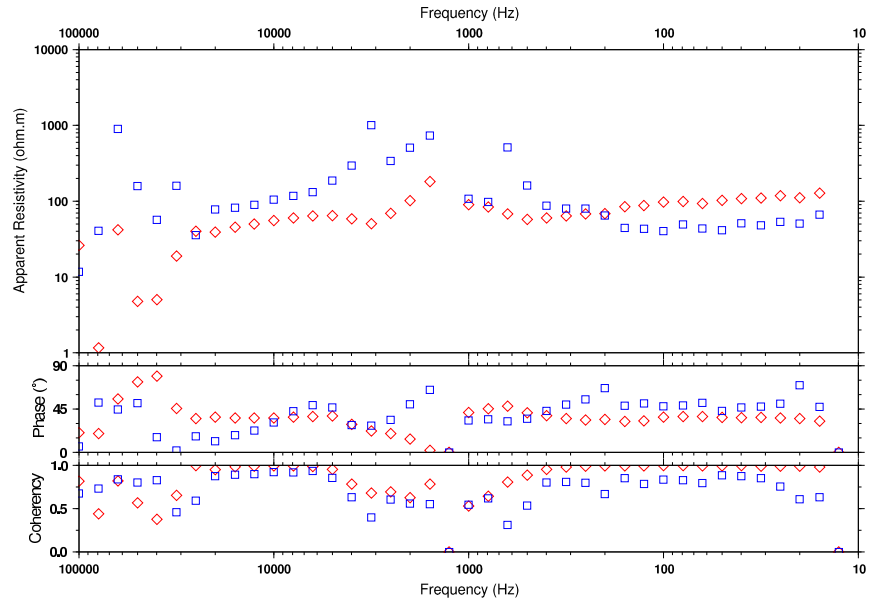
SVNE 00400m 019 - Scalar Res., Coherency, Phase (diamond=ExHy; square=EyHx)



SVNE 00800m 036 - Scalar Res., Coherency, Phase (diamond=ExHy; square=EyHx)



SVNE 01000m 026 - Scalar Res., Coherency, Phase (diamond=ExHy; square=EyHx)



SVNE 01200m 027 - Scalar Res., Coherency, Phase (diamond=ExHy; square=EyHx)

